AMMRC TR 82-22

ENERGY

CONSERVATION

SINTERED Si_3N_4 FOR HIGH PERFORMANCE THERMOMECHANICAL APPLICATIONS

W.D. Pasco and C.D. Greskovich

April 1982

GENERAL ELECTRIC COMPANY
CORPORATE RESEARCH AND DEVELOPMENT
SCHENECTADY, NEW YORK 12301

Final Report-1 January 1981 to 1 January 1982

Contract DAAG46-81-C-0029

Prepared for
ARMY MATERIALS AND MECHANICS RESEARCH CENTER
Watertown, Massachusetts 02172

under AMMRC/DOE Interagency Agreement EC-76-A-1017-002
Department of Energy
Division of Transportation Energy Conservation
Heat Engine Highway Vehicle Systems Program

U. S. DEPARTMENT OF ENERGY

Division of Transportation Energy Conservation

The findings in this report are not to be construed as an official Department of the Army position, unless so designated by other authorized documents.

Mention of any trade names or manufacturers in this report shall not be construed as advertising nor as an official indorsement or approval of such products or companies by the United States Government.

DISPOSITION INSTRUCTIONS

When this report is no longer needed, Department of the Army organizations will destroy it in accordance with the procedures given in AR 380-5. Navy and Air Force elements will destroy it in accordance with applicable directions. Department of Defense contractors will destroy the report according to the requirements of Section 14 of the Industrial Security Manual for Safeguarding Classified Information. All others will return the report to Army Materials and Mechanics Research Center.

Unclassified

SECURITY CLASSIFICATION OF THIS PAGE *(When Data Entered)*

REPORT DOCUMENTATION PAGE

READ INSTRUCTIONS BEFORE COMPLETING FORM

1. REPORT NUMBER AMMRC TR 82-22	2. GOVT ACCESSION NO.
3. RECIPIENT'S CATALOG NUMBER	
4. TITLE *(and Subtitle)* Sintered Si_3N_4 For High Performance Thermomechanical Applications	5. TYPE OF REPORT & PERIOD COVERED Final Report 1 Jan. 1981 – 1 Jan. 1982
	6. PERFORMING ORG. REPORT NUMBER SRD-82-045
7. AUTHOR(s) W.D. Pasco and C.D. Greskovich	8. CONTRACT OR GRANT NUMBER(s) DAAG46-81-C-0029
9. PERFORMING ORGANIZATION NAME AND ADDRESS General Electric Company Corporate Research and Development Schenectady, New York 12301	10. PROGRAM ELEMENT, PROJECT, TASK AREA & WORK UNIT NUMBERS Interagency Agreement EC-76-A-1017-002
11. CONTROLLING OFFICE NAME AND ADDRESS Army Materials and Mechanics Research Center ATTN: DRXMR-K Watertown, Massachusetts 02172	12. REPORT DATE April 1982
	13. NUMBER OF PAGES 54
14. MONITORING AGENCY NAME & ADDRESS *(if different from Controlling Office)*	15. SECURITY CLASS. *(of this report)* Unclassified
	15a. DECLASSIFICATION/DOWNGRADING SCHEDULE

16. DISTRIBUTION STATEMENT *(of this Report)*

Approved for public release; distribution unlimited.

17. DISTRIBUTION STATEMENT *(of the abstract entered in Block 20, if different from Report)*

18. SUPPLEMENTARY NOTES

19. KEY WORDS *(Continue on reverse side if necessary and identify by block number)*

Gas Pressure Sintering	Oxygen
Silicon Nitrides	High Temperature
Beryllium Compounds	Ceramic Materials

20. ABSTRACT *(Continue on reverse side if necessary and identify by block number)*

The gas pressure sintering (GPS) process for dense (>99%) Si_3N_4 containing ~7 wt% $BeSiN_2$ and 7 wt% SiO_2 as sintering aids was scaled-up to develop a property data base for use in thermomechanical applications at high (~1300 °C) temperatures. The fracture strength in 3-pt bend for test bars ~0.6 cm × 0.6 cm × 4.5 cm long was ~440 MNm^{-2} (63,700 psi) for a span length of 3.8 cm. There was little drop (<15%) in high temperature strength at 1400 °C in air. The creep resistance was outstanding at 1300 to 1400 °C, as evidenced by creep rates of ~$4 \times 10^{-5} h^{-1}$ for a stress of 207 MPa (30,000 psi) at 1400 °C

DD FORM 1 JAN 73 1473 EDITION OF 1 NOV 65 IS OBSOLETE

Unclassified

SECURITY CLASSIFICATION OF THIS PAGE *(When Data Entered)*

SUMMARY OF IMPORTANT RESULTS

The gas pressure sintering (GPS) process for sintered Si_3N_4 was scaled-up to develop a property data base for use in thermomechanical applications. Optimization of sintering conditions and problems with large BN crucibles in a large pressure furnace (9 cm dia x 12.5 cm high hot zone) are described.

Room temperature fracture strength for GPS Si_3N_4 containing $\sim$ 7 wt% $BeSiN_2$ and $\sim$ 7% SiO_2 as sintering aids was measured on sample sizes having a stressed volume more than 10 times larger than those investigated during last year's program. The average fracture strength in 3-pt bend for test bars $\sim$ 0.6 cm x 0.6 cm x 4.5 cm in dimensions was $\sim$ 440 MNm^{-2} (63,700 psi) for a span length of 3.8 cm and the Weibull modulus was $\sim$ 8. A 25% increase in room temperature fracture strength can be realized if Si_3N_4 test bars are given a post sintering anneal at 1600°C in N_2 followed by oxidation in air at 1300°C for 1 hr before mechanical testing. The fracture strength of GPS Si_3N_4 does not change much from room temperature to $\sim$1400°C, but at 1500°C the fracture strength is about 50% of its room temperature value. Fracture origins were generally associated with porous regions within the bulk of the specimens. Average fracture strengths near 700 MNm^{-2} at room temperature are expected for GPS Si_3N_4 with a fine grain, fine-pore ($< 5\ \mu m$) microstructure.

The creep behavior of GPS Si_3N_4 was outstanding in air at temperatures between 1300 and 1400°C under high applied stresses between 207 MPa (30,000 psi) and 345 MPa (50,000 psi). The creep rates after $\sim$150 h of testing were $\sim 4 \times 10^{-5} h^{-1}$ for a 207 MPa stress at 1400°C and $\sim 2 \times 10^{-6}\ h^{-1}$ for a 345 MPa stress at a temperature of 1300°C. A long term creep experiment at 1300°C showed that GPS Si_3N_4 could survive an applied stress of 345 MPa (50,000 psi for 650 h without failure, a finding not previously demonstrated. The total creep strain on this crept bar was estimated to be only 0.11%.

The oxidation resistance of GPS Si_3N_4 was extremely high after long exposures in flowing oxygen at temperatures between 1000 and 1400°C. A protective, thin oxide layer of α-cristobalite was detected on GPS Si_3N_4 samples oxidized for long (500 h) times at 1300°C. The parabolic rate constants were 7.4 x 10^{-13} and 2.1 x 10^{-12} $kg^2m^{-4}s^{-1}$ at 1300 and 1405°C, respectively, corresponding to an oxidation rate $\sim$2-3 orders of magnitude lower at 1400°C than that for commercially hot-pressed NC-132 Si_3N_4. The activation energy for oxidation between 1300 and 1400°C was calculated to be 209 kJ/mole.

A long oxidation test carried out at 1000°C for 200 h showed no detectable oxidation and confirmed that GPS Si_3N_4 does not undergo catastrophic oxidation similar to that observed in some hot pressed forms of Y_2O_3-containing Si_3N_4 ceramics.

A gas burner rig test was conducted for 525 h at 1200°C using an air-to-fuel ratio of 7.5/1 to determine the possible loss of beryllium from dense (>99%) GPS Si_3N_4 when the flame impinged on the ceramic. Based on the amount of Be detected in the residue collected at the exhaust end of the burner rig, it was calculated that the exit gas contained 6 parts per billion by weight of Be.

Finally, we have demonstrated that injection-molded Si_3N_4 (with $BeSiN_2$ and SiO_2 additives), produced by K. Styhr at AiResearch can be sintered to full density by the GPS process.

FOREWORD

This development work has been sponsored by the Army Materials and Mechanics Research Center under AMMRC/DOE Interagency Agreement EC-76-A-1017-002 as part of the DOE, Division of Transportation Energy Conservation, Highway Vehicle Systems Heat Engine Program and carried out in the Physical Chemistry Laboratory of the General Electric Research and Development Center, Schenectady, New York, under Contract DAAG-46-81-0029 during the period January 1981 - January 1981. Mr. George Gazza was the Program Monitor.

The authors would like to acknowledge Dr. R.J. Charles for his overall guidance of this program, D. Polensky for considerable help with ceramic processing and heat treatments, C. O'Clair for this ceramic processing skills, and the Materials Characterization Laboratory for x-ray and microscopy work.

I. INTRODUCTION

Silicon nitride based materials are currently receiving a great deal of attention for potential application in small automotive gas turbines to operate eventually at turbine inlet temperatures of $\sim 1370^{\circ}C$ ($\sim 2500^{\circ}F$). Perhaps the most demanding ceramic part contemplated for use is the rotor, approximately 12.5 cm in diameter and capable of high strength (690 MN/m^2) to about $1000^{\circ}C$, good oxidation and creep resistance to about $1300^{\circ}C$, and having the potential for mass production into near-net-shapes. Until recently, the only two forms of Si_3N_4 available for use are reaction-bonded and hot-pressed Si_3N_4. Although reaction-bonded Si_3N_4 can be mass produced conveniently into intricate shapes and exhibit adequate creep properties, it suffers from poor oxidation behavior (because of the high residual porosity of $\sim 15\%$) and low fracture strength (typically < 500 MN/m^2). Hot pressed Si_3N_4 is difficult to mass produce into complex shapes at reasonable costs and usually has poor creep behavior at $T < 1200^{\circ}C$. Because of the inadequacies of reaction-bonded and hot-pressed forms of Si_3N_4, the development of sintered Si_3N_4 was cited as a priority goal for materials development for small automotive gas turbine engines in 1974[1]. In fact, it was in 1974 that developments in SiC[3] and Si_3N_4[3] research led to the fabrication of dense (>90% of the theoretical density) ceramics by the sintering process.

There are a number of difficulties in sintering Si_3N_4 to full density with good thermomechanical properties. Si_3N_4 is a covalently bonded solid ($\sim 70\%$ covalency[4]) and, consequently, a large amount of energy is required for the formation and motion of structural defects which permit sintering by diffusion. Since densification (macroscopic shrinkage) of powder compacts of Si_3N_4 must take place by grain boundary and/or volume diffusion mechanisms, chemical additives and high temperatures are usually used to increase the densification kinetics by

increasing the effective diffusion coefficient of the rate-limiting species (generally assumed to be N, based on recent self-diffusion measurements[5]). In addition, submicrometer particle sizes are usually employed to increase the sintering kinetics as well as the rate of chemical reaction between the additive phases(s) and the Si_3N_4 particles.

Typically, the chemical additive selected for Si_3N_4 forms a liquid (glassy) phase during sintering by reacting with SiO_2 (and impurities) on the particle surfaces of α-Si_3N_4 (low temperature polymorph) and transforms them into β-Si_3N_4, probably via a solution-reprecipitation process[6-9]. This SiO_2-rich glassy phase resides along the β-Si_3N_4 grain boundaries and degrades the thermo-mechanical properties via grain boundary sliding[10-11] and intergranular creep cavitation[11-13] mechanisms. Improved mechanical properties of dense Si_3N_4 are anticipated by reducing the amount of residual glassy phase by composition control and subsequent induced crystallization and/or by increasing the viscosity of the glassy phase. However, the sintering (densification) rate of Si_3N_4 is typically decreased by reducing the amount of glassy phase and by increasing its viscosity. To counterbalance this limited sinterability, higher temperatures (>1800°C) may be used, but then introduce the problem of thermal decomposition of Si_3N_4[14] and the glassy phase, resulting in density regression and a low density of the final product. Recent experiments[15] have shown, however, that thermal decomposition can be minimized or controlled by using increased N_2 pressures up to$\sim$ 2 MPa. It appears that the development of fully-dense, sintered Si_3N_4 depends strongly on the competition between the rates of densification and thermal decomposition. This implies the acceptance of the inconvenience of sintering Si_3N_4 at high temperatures and high N_2 pressures, an unusual practice in ceramics.

Details of our last year's work on the development of a gas pressure sintering (GPS) process for making dense (>99%), sintered Si_3N_4 with outstanding thermo-

mechanical properties were presented in a Final Technical Report[18]. This report showed that small (0.5 to 5g) samples of Si_3N_4, containing 0.5-1.0 wt% Be and 2.5-3.7 wt% O, could be sintered reproducibly to < 99% relative density by a two-step (GPS) process. The average 3-pt bend strength of test bars 0.25 x 0.25 x 1.9 cm span length was 600 MPa at room temperature and ∿550 MPa at 1300°C in air. The creep resistance of GPS Si_3N_4 was excellent and exhibited steady state creep rates of only 4.6×10^{-7} and 6.9×10^{-6} h^{-1} at 1300 and 1400°C, respectively, for an applied stress of 69 MPa. The oxidation rate was extremely low between 1000 and 1500°C and was sensitive to furnace impurities. Complex shape demonstration was achieved by the fabrication of modified T-700 blades by slip casting with final sintered densities as high as 98% of the theoretical value.

II. SCOPE OF WORK

The main thrust of the current program is to scale-up the GPS process for the composition of Si_3N_4 containing densification aids of 7 wt% $BeSiN_2$ and 3.4-3.7 wt% oxygen for generation of thermomechanical data for comparison with other high temperature structural materials. Physical and mechanical properties will be determined at room temperature and high temperature, 1300°C. A number of specimens of GPS Si_3N_4 will be sent to AMMRC for additional thermomechanical testing. Finally, gas burner rig studies will be performed to determine the take-up rate of airborne particulate beryllium-containing species from GPS Si_3N_4 by the exhaust gases for operational conditions approximating 1200°C in an oxidizing flame for a test duration of 500 to 1000 hours.

III. EXPERIMENTAL PROCEDURES

A. Preparation of $BeSiN_2$ Additive

The sintering aid, $BeSiN_2$, was prepared by mixing equimolar quantities of Be_3N_2 and Si_3N_4 and reacting according to the equation:

$$Be_3N_2 + Si_3N_4 = 3\ BeSiN_2$$

Typically the starting Be_3N_2 powder is -60 mesh and must be handled in a dry N_2 glove box because of its hygroscopicity. Sylvania SN502 Si_3N_4 powder (specific surface area $\sim$ 4.5 m^2g^{-1}) was used as a source of high purity material. These reactants were mixed in a Nalgene jar mill for 1 hour using heptane and Si_3N_4 grinding media. After mixing, the slurry was dried in the N_2 glove box for about 12 hours and then collected. The dried powder mixture was isostatically pressed at a low forming pressure of $\sim$14 MPa, and then the green slug was placed in a BN crucible for heating. Chemical reaction occurs conveniently at 1600-1700°C for 20 min in 2-3 MPa of N_2 pressure. The resulting powder was confirmed by XRD to be $BeSiN_2$ plus a trace of β-Si_3N_4. A reaction temperature of 1600°C for 40 minutes is preferred because the resulting $BeSiN_2$ powder is softer. Thus far, 80 grams of $BeSiN_2$ powder have been synthesized for our in-house use.

During this program a request for $BeSiN_2$ additive came from Mr. Karsten Styhr who is currently undertaking an injection molding program for promising Si_3N_4 ceramics. He has injection molded General Electric's Si_3N_4 composition into test bars (5.1 cm x 0.3 cm x 0.6 cm) and standard AiResearch turbocharger wheels (T-4 size) 7.5 cm in diameter measured across the blade tips. Consequently over 150 grams of $BeSiN_2$ additive was synthesized for the AiResearch program to help speed-up the fabrication of complex shapes of the GE Si_3N_4 composition.

B. Processing Pure Si_3N_4 Powder

High purity Sylvania SN502 Si_3N_4 powder was selected as the major powder source. It was decided that processed, "pure" Si_3N_4 powder could be used for qualifying the best powder pressing techniques and sizes and shapes of dies used for the scale-up process for sintered Si_3N_4 containing the $BeSiN_2$ additive. Typically, 450 grams of SN502 powder was ball milled for 72 hrs in

a steel mill using hexane as a liquid medium. The milled powder was leached for ∿12 hrs with a 7.4% HCl solution to remove metallic impurities introduced during milling. The "frothy" Si_3N_4 slurry was then washed repeatedly with H_2O until there was no detection of Fe^{2+} ions by the $K_3Fe(CN)_6$ test. The next step involved washing the slurry with acetone to remove the Cl^- ions. This was done until there was a negative test using $Ag(NO_3)$. After the acetone washing was completed, the slurry was dried for ∿12 hrs at room temperature in a ventilated hood. The milled Si_3N_4 powder usually has a specific surface area of ∿10 m^2/g and is typical of a standard sinterable Be-containing Si_3N_4 powder.

C. Processing SN502 Si_3N_4 Containing $BeSiN_2$ Additive

A total of 4 batches of sinterable Si_3N_4 powder were prepared by adding 7 w/o of $BeSiN_2$ as a sintering aid. Three batches were prepared in ∿200 g amounts starting with Sylvania SN502 Si_3N_4 (Lot #04-48) by a process similar to that described above except the $BeSiN_2$ was added prior to milling. The batches were identified as SN502-95, SN502-100, and SN502-105. Batch SN502-105 was leached with solution of 7.4% HCl and 9.1% HNO_3. A fourth batch was prepared using 300 g of SN502 Si_3N_4 (Lot #04-12) which had been previously prepared by the procedure described above which contained no $BeSiN_2$ additive. An addition of 7 w/o $BeSiN_2$ was made by ball milling in a steel mill for 8 hrs. After milling, the powder was leached with a solution of 7.4% HCl and 9.1% HNO_3 followed by the normal washing procedure. This batch was identified as SN502-110. Table I presents the specific surface area (S_s) as determined by single-point B.E.T. nitrogen adsorption method, oxygen content as determined by neutron activation analysis and Fe and Cl content.

Table I

Characterization of Processed SN502 Si_3N_4 Containing $BeSiN_2$ Additive

Batch #	S_s m^2/g	Oxygen w/o	Fe ppm	Cl ppm
SN502-95	10.4	1.54	450	610
SN502-100	11.5	1.69	230	520
SN502-105	10.4	2.12	270	< 70
SN502-110	11.4	3.54	133	N.A.

It has been found that the Cl impurity can be reduced to $\sim$600 ppm by more extensive acetone washing and it can even be reduced to $\sim$100 ppm or less by oxidizing the processed powder at 1000°C for 10 min. Since all sinterable powders receive an oxidation treatment before sintering, extensive acetone washing is not necessary. Similarly, more extensive water washing and leaching can reduce the Fe impurity from 450 to 230 ppm but it was found that a second HCl + HNO_3 leaching step could reduce the Fe impurity to $\sim$ 30 ppm. A typical photomicrograph of the final processed powder (not oxidized) is shown in Fig. 1. The small fraction of elongated particles 1 to 2 m in length is probably associated with the β-Si_3N_4 phase detected by XRD. The SN502 Si_3N_4 powder generally contains 60 to 80% crystalline material, about 92% of which is α-Si_3N_4 and 8% β-form, and the remainder of the powder consists of amorphous Si_3N_4. The majority of Si_3N_4 particles are $\sim$0.2 μm in size, equiaxed and probably of the alpha and amorphous forms.

Some early sintering experiments were carried out using sinterable powders previously produced during last year's program. These processed powder compositions were SN502-23A and SN502-57 and had similar particle sizes, oxygen contents, beryllium contents and impurities as those described above.

D. Powder Forming

Powder compaction was initially achieved by both die and isostatic pressing of powders containing no binders or lubricants. Typically, a compact was first die-pressed in a double-acting die at a pressure of $\sim$28 MPa and then pressed isostatically at $\sim$200 MPa. Several sizes and shapes of green compacts were investigated. Small cylindrical-shaped green compacts having weights of $\sim$1 g and dimensions of $\sim$1 cm in diameter x $\sim$1 cm high were formed for many qualification runs used to optimize the sintering conditions. Large cylinders of 15 g and having dimensions of $\sim$2 cm in diameter and $\sim$3.3 cm long were fabricated to compare sintering results for material fired in the large sintering furnace with that for material sintered in the small furnace used last year. Mechanical test bars were prepared from green compacts having a weight of $\sim$5 g and dimensions of $\sim$6 cm x 1 cm x 1 cm. Several large disks $\sim$5 cm in diameter x 1 cm high, were formed to show size capability achievable by the pressing method described.

It was found that the green density of compacts could be increased by the addition of lubricants. The lubricant solution used consisted of 150 cc 2-propanol, 50 cc dibutyl phthalate, 3 cc oleic acid and 8 g stearic acid. The lubricant was mixed in with the powder in a mortar and pestle and the propanol was allowed to evaporate. After evaporation of the propanol, the other constituents remained in the powder and the weight percent lubricant to be reported is based on the constituents that actually remain in the powder. Utilization of the pressing procedure reported above, it was found that compacts containing no lubricant, 5 w/o lubricant and 10 w/o lubricant achieved green densities of 48.0%, 49.2% and 52.7% of theoretical (3.18 g/cm^2). The reported green densities were determined after removal of the lubricant by heat treating at 600°C in air for 1 hr.

E. Oxidation of Powder Compacts

The processed Si_3N_4 powders with 7 w/o $BeSiN_2$ contain insufficient oxygen content for high sinterability. A controlled oxidation process[18] previously established permitted oxygen take up and good distribution of this densification aid. Generally, the compacts of the initial composition studied herein require $\sim$ 3.2-3.7 w/o oxygen for high sinterability. Previous discussion of the oxidation process was based on the oxidation of Si_3N_4 by the reaction:

$$Si_3N_{4(s)} + O_{2(g)} = 3\ SiO_{2(s)} + 2\ N_{2(g)}$$

Based on weight gain measurements, the total oxygen content, O_T, of an oxidized compact is determined from the equation[19]:

$$O_T = O_i + 2.4\ (\Delta W/W_f \times 100)$$

where O_i is the initial oxygen content before oxidation and $\Delta W/W_f$ is the weight gain during oxidation relative to the final weight, W_f.

Another possibility which must be considered is the oxidation of $BeSiN_2$. Experiments were done to determine the relative rates of oxidation of $BeSiN_2$ and Si_3N_4 at 1045°C for 2 hrs. in air. The $BeSiN_2$ was used in the as-reacted state (preparation described previously) and as such should have had a lower surface area than the Si_3N_4 which had been milled for 72 hrs., leached and washed. After oxidation, the $BeSiN_2$ gained 1.35 w/o and the Si_3N_4 gained 0.1 w/o, which indicates that $BeSiN_2$ oxidizes more rapidly than Si_3N_4.

X-ray diffraction of the oxidized $BeSiN_2$ indicates that the most probable oxidation product is $BeSiO_3$ by the reaction:

$$BeSiN_{2(s)} + 3/2\ O_{2(g)} = BeSiO_{3(s)} + N_{2(g)}$$

The appropriate equation for total oxygen content is:

$$O_T = O_i + 2.33\ (\Delta W/W_f \times 100)$$

Since this equation is almost identical to that given for oxidation of Si_3N_4, the oxygen contents previously reported should be quite accurate.

The furnace used for the oxidation treatment was Kanthal heated and has a hot zone of 20 cm x 20 cm x 10 cm. It has the capability of a rapid heating rate of $\sim$1000°C/h. The oxidation behavior of compacts of Batch SN502-95 was studied and is presented in Figure 2. The total oxygen content for compacts held for 1 hr at temperature rises markedly from $\sim$2.8 w/o at 950°C to $\sim$3.8 w/o at 1025°C. The percent weight gain experienced by 1 g and 15 g compacts was essentially identical, indicating that sample size effects should be minimal and that gradients in oxygen content across the sample should not be a problem with increasing sample size.

F. Equipment Set-up and Calibration

The high temperature creep rig was rebuilt to insure reliable operation for long term creep experiments. The sensitivity of this creep system was calibrated with sintered β-SiC specimens at 1300°C and 1450°C. The results showed that the creep rig can reliably measure creep rates as low as 1×10^{-6} h^{-1}.

The large high temperature high pressure sintering furnace was debugged and the true temperature was determined at 3.6 MPa N_2 pressure by the melting point of alumina. It was determined that a correction factor of 115°C above the optical pyrometer reading was required for true temperature. The scale-up sintering furnace was checked out to 2200°C with N_2 pressures up to 7.1 MPa.

IV SCALE UP OF THE GAS PRESSURE SINTERING PROCESS

A. Initial Experiments

Initial sintering experiments were conducted to verify that the large high pressure furnace (9 cm diameter and 12.5 cm high hot zone) was capable of producing high density (>99%) Si_3N_4 by the GPS process. Powder compositions SN502-23A and SN502-57 which were previously sintered to

>99% density in the small N_2 pressure furnace were investigated. Small (∿2 g) compacts of SN502-23A with an oxygen content of 3.6 w/o were sintered to densities of 98.5% by the standard 2 step process in which∿ 2.3 MPa of N_2 was applied at 2140°C for 15 min followed by 6.9 MPa of N_2 at 2005°C-2055°C for 15 minutes. The weight loss of the ∿98.5% dense sample was 1.3%.

Since relatively high density (98.5%) was achieved in the high pressure furnace, a new batch, SN502-95, containing 7 w/o $BeSiN_2$ was examined. Sintering experiments were made in the large high pressure furnace with 15 g compacts (1.9 cm dia x 3.3 cm high) and 3.9 wt% oxygen. The specimens were placed in a BN crucible (2.1 cm ID x 4.6 cm high) which had been baked out at 1955°C for 60 min in N_2 to remove volatile impurities. No specimens had been fired in the new crucible which was the same size as the old BN crucible used to fire the SN502-23A samples discussed above. The first specimen (SN502-95-4) achieved a fired density of 94.8%. Accurate temperature measurement was not possible due to the growth of a fibrous deposit in the SiC sight tube. Removal of the fired specimen from the crucible revealed that a white deposit, identified by XRD to be BN, was present on the surface of the sample, especially on the ends. The second firing (SN502-95-5) employed ∿20°/min heating rate to a 20 minute isothermal hold at 2145°C under 2.5 MPa of N_2 and a 20 minute isothermal hold at 2035°C under 6.9 MPa of N_2. The relative density of this sample was 93.6%. The specimen did not display as much of the white deposit as did the previously fired sample but definite crucible effects were apparent. Densification of the sample was impeded on the end in contact with the BN crucible. The bulk of the compact experienced∿ 20% linear shrinkage compared to 17.4% where contact was made with the BN. All subsequent firings utilized a sintered

Si_3N_4 setter between the sample and the crucible. A ceramographic section of the sample revealed that a higher density region existed at the surface, indicating too rapid a heating rate with concomitant temperature non-uniformity throughout the sample. Subsequent firings revealed that a heating rate of 8-10°C/min above 1750°C gave uniform microstructural appearance with no obvious density differences from center to surface of the sample.

Due to the low (93.6%) density of specimens fired to 2145°C in the first step of the GPS process, it was necessary to increase this temperature. A 15 g compact (SN502-95-7) with 3.6 w/o oxygen was fired at 2175°C in 2.2 MPa of N_2 for 20 minutes in the first step and 2085°C in 6.9 MPa of N_2 for 20 minutes in the second step and achieved a density of 98.6% with a weight loss of 0.62%. Another sample, (SN502-95-8) was isostatically pressed at 345 MPa (50,000 psi) instead of the normal 207 MPa (30,000 psi) and was fired at 2130°C in 2.3 MPa of N_2 for 20 minutes in the first step and 2090°C in 6.9 MPa of N_2 for 20 minutes in the second step. This sample achieved a fired density of 99.0% and a weight loss of 0.19%. The high density achieved for the 15 g sample represents the attainment of state-of-the-art that was accomplished in the small high N_2 pressure furnace of the previous AMMRC contract.

Sintering experiments were conducted on bars (5.8 cm x 1 cm x 1 cm) which were cold pressed at $\sim$24 MPa and isostatically pressed at 207 MPa. A bar (SN502-95-10) was fired in a vertical position in the furnace at 2205°C, 2.3 MPa, 20 minutes in the first step and 2085°C, 6.9 MPa, 20 minutes in the second step. The specimen was observed to exhibit substantial thermal decomposition on the top 1/3 of the bar but not on the bottom. It was apparent that although the tip of the SiC sight tube was fully in the hot zone, the specimen was not. Additional porous carbon was placed in the furnace in

order to raise the specimen further into the hot zone. To prevent thermal decomposition of the specimen, the firing temperature was decreased. A 6 g bar (SN502-95-11) was fired at 2145°C, 2.1 MPa, 30 minutes in the first step and 2045°C, 6.9 MPa, 30 minutes in the second step thus attaining a final density of 98.8% and a weight loss of 0.98%.

The initial sintering experiments described above served the purpose of debugging the large furnace and establishing the procedures for accurate temperature measurement, having the sample placed in a uniform hot zone, and the general time, temperature and pressure parameters required to produce high density sintered Si_3N_4.

B. Effect of Temperature on the Second Step of the GPS Process

Although the effect of pressure on the densification kinetics during the second step of the GPS process had been investigated during the last contract, the effect of temperature had not been fully explored. To better understand the second step of the GPS process, a series of ∿1 g cylindrical specimens (0.9 cm dia x 1.0 cm high) were fired. The conditions of temperature, pressure and time for the first step were kept constant at 2145°C in 2.2 MPa of N_2 for 30 minutes and yielded a final density of 92.3% and weight loss of 0.44%. Specimens were fired individually with the parameters of the first step constant and the parameters of the second step varied but only with respect to temperature. The pressure was maintained at 2.2 MPa rather than increasing it, and the isothermal soak time was 30 minutes. The temperature of the second step, final density and weight loss are summarized in Table II.

Table II

Sample #	Second Step T,P,t	ρ_f, %	$\Delta W/W_o$, %
SN502-95-12	No second step	92.3	0.44
SN502-95-13	2145°C, 2.2 MPa, 30 min	93.6	0.83
SN502-95-14	2045°C, 2.2 MPa, 30 min	97.9	0.91
SN502-95-15	1995°C, 2.2 MPa, 30 min	98.7	1.23
SN502-95-16	1955°C, 2.2 MPa, 30 min	99.9	1.77
SN502-95-17	1905°C, 2.2 MPa, 30 min	93.8	2.18
SN502-95-18	1955°C, 2.2 MPa, 60 min	94.8	2.84

It was observed that the first step of the process yielded a density of 92.3%, for which closed porosity was obtained. By increasing the hold time from 30 to 60 minutes under the defined condition of the first step, the density only increased to 93.6% and the weight loss doubled. By maintaining pressure constant and decreasing the temperature the density reached a maximum of 99.9% at 1955°C. The density was observed to decrease as temperature was decreased to 1905°C. In addition, a specimen was held at 1955°C, the temperature of maximum density, for 60 minutes rather than 30 minutes and the density decreased to 94.8% and the weight loss increased from 1.77 to 2.84%. This result is not understood and the experiment should be repeated to verify the effect.

The point to be emphasized is the unusual result of increasing density and weight loss with decreasing temperature. The first step of the sintering process requires heating the specimen containing $\sim$ 7 w/o $BeSiN_2$ and $\sim$ 7 w/o SiO_2 to 2145°C, in 2.2 MPa of N_2 for 30 minutes. This treatment prevents the thermal decomposition of Si_3N_4 due to high N_2 pressure while permitting a liquid phase of unknown composition to form. The liquid is believed to be a beryllium-silicon-oxynitride initially, which promotes liquid phase sintering.

As the Si_3N_4 dissolves, transports through the liquid and precipitates out, the compact densifies and decreases its specific surface area. It is believed that the precipitated β -Si_3N_4 is in fact a β-Si_3N_4 solid solution containing significant amounts of Be and O as confirmed by x-ray analysis. It has been observed that the densification proceeds to a "limiting" density of $\sim$93.6% after 60 minutes at 2145°C. Further increases in temperature may provide additional liquid phase to permit further densification, but probably at the expense of the mechanical properties due to increased grain size.

To more fully understand the effect of increasing density with decreasing sintering temperature at constant pressure in the second step of the GPS process, the sintered specimens shown in Table II were examined with SEM. The sintered samples were sectioned, metallographically polished and chemically etched prior to SEM examination. The etchant was a fused salt containing 4:4:1 parts by weight of NaOH, KOH and LiOH, respectively, and samples were etched for 30 minutes at 200°C. Figure 3 shows the microstructure of sample SN502-95-12 at 10,000 X which had been fired at 2145°C, 2.2 MPa, 30 min. This contrasts with Figure 4 which shows the microstructure of SN502-95-13 which had been fired at 2145°C, 2.2 MPa, 60 minutes. The most prominent observation is the large increase in grain size caused by a 60 minute soak over the 30 minute soak. It is believed that the grain growth and concomitant pore coalescence[18] are the causes of the observed "limiting" density ($\sim$93.6%) which occurs when the 2145°C isothermal hold is extended to longer times. The increase in grain size indicates that the time and temperature parameters of the first step of the GPS process are important in controlling the final grain size. Figure 5 shows the microstructure of SN502-95-14 which was fired at 2045°C, 2.2 MPa, 30 min. in the second step and achieved a density 97.9%. The grain size is smaller

than shown in Figure 4 indicating that dropping the soak temperature in the second step not only increases the fired density but serves to maintain a smaller final grain size. Figure 6 shows the microstructure of SN502-95-15 which was fired at 1995°C, 2.2 MPa, 30 min. in the second step and shows a grain size which more closely approximates that obtained in the first step of the GPS process. (Fig. 3). The same observation is apparent in Figure 7 which shows SN502-95-16 which was fired at 1945°C, 2.2 MPa, 30 min. and achieved a density of 99.9%. By decreasing the soak temperature in the second step to 1905°C, the density dropped to 93.8% and no further gains were available by decreasing the soak temperature.

In addition to the decrease in grain size with decreasing soak temperature in the second step, it was also observed that the etching of the grain boundary became less pronounced thus indicating the presence of a smaller amount of liquid phase at the lower temperature. This is consistent with the results of Huseby et al.[20] which indicate a greater solubility of Be and O in the β-Si_3N_4 solid solution with decreasing temperature, which would cause the liquid phase to "dry up" as it dissolves into the β-Si_3N_3 lattice. Lattice parameter determinations of the β-Si_3N_4 solid solutions were conducted by Debye-Scherrer analysis to see if this effect could be observed. The results shown in Table III indicate that no clear trend was observed.

Table III

Lattice Parameter Determination of the β-Si_3N_4 Solid Solution

Sample #	a, Å	c, Å
SN502-95-13	7.5890 ± 0.0002	2.9012 ±0.0008
SN502-95-14	7.5876 ± 0.0019	2.9015 ± 0.0007
SN502-95-15	7.5880 ± 0.0016	2.9015 ± 0.0006
SN502-95-16	7.5878 ± 0.0012	2.9017 ± 0.0004
SN502-95-17	7.5866 ± 0.0016	2.9013 ± 0.0006
SN502-95-18	7.5877 ± 0.0008	2.9018 ± 0.0003

The reason for the increase in fired density with decreasing soak temperature at constant pressure during the second step of the GPS process is still not understood.

One possibility for the increased densification is the solubility of the N_2 trapped in the closed pores with decreasing temperature. If the N_2 solubility in the liquid phase increases with decreasing temperature then the gas pressure in the pores will decrease and thus remove the barrier to pore closure and densification will proceed. The equilibrium composition of the liquid phase as a function of temperature is not known and therefore the discussion must be speculative in nature. If it is assumed that the equilibrium liquid composition shifts from oxygen-rich toward nitrogen-rich as temperature decreases, then the nitrogen in the pores would be dissolved into the liquid phase and some Be and O should dissolve into the β-Si_3N_4 solid solution. It may be possible that insufficient N_2 exists in the porosity to satisfy the equilibrium composition and that O_2 must be expelled from the liquid phase. It is clear from neutron activation analysis shown in Table IV that with decreasing soak temperature in the second step of the GPS process, oxygen is lost from the compact. Thermodynamic considerations suggest that

the oxygen evolves from the compact in the form of SiO(g). These thermodynamic considerations are supported by the fact that SiC fibers were observed to grow on the outside of the crucible where the crucible cover screws into the crucible, thus indicating that a silicon-containing vapor species evolves from the compact and reacts with a C-bearing vapor species. Table IV presents the sample #, the oxygen content of the sintered specimen, the observed weight loss and the expected weight loss when calculated as SiO(g).

Table IV

Results of Oxygen Analysis

Sample #	Oxygen w/o	$\Delta W/W_o$,% observed	Oxygen w/o	$\Delta W/W_o$, SiO
SN502-95-12	3.99	0.44	0	.44
SN502-95-13	3.98	0.83	0.01	.47
SN502-95-14	3.64	0.91	0.35	1.40
SN502-95-15	3.45	1.23	0.54	1.93
SN502-95-16	3.36	1.77	0.63	2.18

The calculated weight loss as SiO(g) was determined by considering that SiO contains 36.3 w/o oxygen and 63.7 w/o silicon. The observed weight loss for SN502-95-12 was 0.44 w/o and served as a baseline, and calculated oxygen w/o was referenced to this sample.

The weight loss due to SiO loss was calculated from

$$(\Delta W/W_o)_{SiO} = 0.44 + \frac{\text{oxygen\%}}{0.363} \quad .$$

Table IV shows that the weight loss calculated as SiO loss is greater than the observed weight loss but follows the same trend. If N_2 is in fact soluble in the liquid phase then a weight gain due to N_2 dissolution may account for the discrepancy. It is emphasized that the above discussion is speculative and open to further reasoning as more data becomes available.

A Be analysis was conducted on the sintered specimens to determine if any Be was lost. Due to difficulty encountered when trying to dissolve the specimens the analysis gave very erratic results and are considered inaccurate. The results are presented in Table V.

Table V

Results of Beryllium Analysis

Sample #	Be w/o
SN502-95-12	0.49
SN502-95-13	0.65
SN502-95-14	0.57
SN502-95-15	0.72
SN502-95-16	0.67
SN502-95-17	0.74
SN502-95-18	0.61

Although the details of why dropping the soak temperature in the second step of the GPS process are not understood, it is clear that it is beneficial to the sintering process.

C. Effect of Soak Temperature in the 1st Step of the GPS Process on Density Using the 2-Step GPS Process

Sintering experiments were conducted on Batch SN502-100 to determine how low the soak temperature in the first step of the GPS process could be and still obtain closed porosity. It is the sintering time and temperature in the first step which predominantly controls the final grain size of the sintered specimen. From the standpoint of achieving the highest possible modulus of rupture, it is essential to minimize the final grain size. It was anticipated that if closed porosity could be achieved in the first step then the application of high N_2 pressure in the second step would result in pore closure and a high

density specimen. Closed porosity occurs at ∿ 92% density and the results of the sintering experiments are presented in Table VI.

Table VI

Effect of Sintering Temperature in the First Step of the GPS Process on Density

Sample #	Temp. °C	Pressure psi	Soak Time min	ρ_f%	$\Delta W/W_o$%
SN502-100-2	2030	320	30	93.3	0.96
-3	1980	315	45	93.0	0.98
-5	1960	312	60	91	1.12
-4	1940	305	60	85	0.90

It was observed that a sintering temperature of at least 1980°C in the first step was required to obtain closed porosity. A specimen (SN502-100-9) was then fired at 2000°C for 30 minutes under 315 psi of N_2 in the first step and 1945°C for 30 minutes under 1000 psi of N_2. The fired specimen had a density of 93.0% and a weight loss of 1.52%. Although the specimen had achieved closed porosity in the first step, it did not go to full density upon application of high pressure. It was again observed that the weight loss increased with decreasing temperature in the second step. A series of experiments was conducted wherein the soak temperature in the first step was increased and the conditions in the second step were kept constant at 1950°C for 30 minutes under 1000 psi N_2. The results are presented in Table VII which shows that by increasing the sintering temperature in the first step to 2095°C it is possible to attain a fired density of > 99%.

Table VIII

Sample #	1st Step	2nd Step	ρ_f%	$\Delta W/W_o$%
SN502-100-9	2000°C, 30 min, 310 psi	1945°C, 30 min, 1000 psi	93.0	1.52
-10	2035°C, 30 min, 320 psi	1950°C, 30 min, 1000 psi	96.5	1.76
-11	2060°C, 30 min, 320 psi	1950°C, 30 min, 1000 psi	98.8	1.91
-13	2095°C, 30 min, 350 psi	1950°C, 30 min, 1000 psi	99.1	2.37

It was observed that the soak temperature in the first step must be $\sim$100°C above the temperature at which closed porosity occurs if 99% density is to be realized in the second step. The reason for this is not totally clear but it is believed to be associated with the amount and/or composition of the liquid phase developing at these high temperatures. Since there is no phase diagram available for this system at high temperature, the liquid phase contains light elements, and the grain boundary phase is extremely thin, analysis of the situation is very difficult.

D. Crucible Effects

It was mentioned previously that firing specimens in "unconditioned" BN crucibles results in the deposition of BN on the specimen. After a few firings of 15 g samples (1.9 cm dia x 3.3 cm high) in a small BN crucible (2.1 cm I.D. x 4.6 cm high) the BN deposition on the sample ceased and uniform high density samples were obtained. The same situation does not hold however when firings are conducted in a large (6.6 cm I.D. x 6.5 cm high) BN crucible.

The sintering experiments discussed in the previous section which were directed toward an understanding of the second step of the GPS process utilized $\sim$1 g cylindrical specimens (0.9 cm dia x 1.0 cm high) contained in a BN crucible of dimensions, 2.1 cm I.D. x 4.6 cm high. The surfaces of the fired specimens were the characteristic dark grey color of dense Si_3N_4 with no evidence of BN deposition. Several firings were done at 2145°C, 2.2 MPa,

30 min. in the first step and 1945°C, 2.2 MPa, 30 min. in the second step in a larger BN crucible (6.6 cm I.D. x 6.5 cm high). After firing, the 1 g cylindrical specimen had a white deposit on the surfaces which was subsequently identified by XRD to be BN. All specimens had been placed on a sintered Si_3N_4 setter and the surface in contact with the setter was dark grey and underwent the expected shrinkage. The exposed surfaces did not densify fully as evidenced by the flared shape of the fired cylinder. In addition, a substantially higher weight loss was observed; 1.8 w/o in the small crucible versus 4 w/o in the large crucible, and a density decrease from 99.9% to 93%.

To insure that all impurities were out of the large crucible and that it was properly conditioned, the crucible was heat treated at 2205°C, 2.4 MPa for 60 minutes. A small∿1 g sample was fired and the BN deposition persisted. A second conditioning treatment involved placing 10 g of SN502 Si_3N_4 containing no additives in the crucible and repeating the high temperature heat treatment. A sintering experiment was subsequently performed whereby a specimen was placed in the large BN crucible. A second specimen enclosed in the small crucible with lid on was also placed in the large crucible. Then, the lid for the large crucible was screwed on. Sintering was performed at 2145°C, 2.2 MPa, 30 minutes in the first step and 2005°C, 3.5 MPa, 30 minutes in the second step. The specimen in the small crucible achieved a fired density of 97.1% and a weight loss of 1.46%, whereas the specimen in the large crucible had a density of 92.9%, a weight loss of 4.5% and was coated again with BN. This experiment indicated that the problem may be associated with crucible-to-sample volume ratio. Since the N_2 pressure and apparent firing temperatures must be the same for both crucibles, it was speculated that enhanced loss of $SiO_{(g)}$ from the sample

occurs in the large crucible. If the $SiO_{(g)}$ pressure rises to some near equilibrium value then the larger volume crucible requires a greater weight loss. Supporting evidence of $SiO_{(g)}$ loss is provided by the β-SiC fibers which were observed to grow around the threads of the crucible lid.

An experiment was conducted whereby SiO powder (0.06 g) was placed in the bottom of the large BN crucible in addition to the 1 g Si_3N_4 (SN502-95-27) specimen which was on a sintered Si_3N_4 setter. The sample was fired at 2095°C, 2.2 MPa, 20 minutes and experienced a 4.5% weight loss, distortion and a white deposit on the surfaces. Again the β-SiC fibers were observed around the crucible lid and there was no evidence of the SiO powder in the crucible. It appears that increasing the vapor pressure of $SiO_{(g)}$ in the crucible does not suppress the weight loss nor the transport of BN from the crucible to the sample.

Another unsuccessful approach toward suppression of the BN transport and sample weight loss was to paint a slurry of SN502 Si_3N_4 on the inside of the crucible. After coating the crucible with Si_3N_4 and drying overnight at 150°C a sample (SN502-95-28) was fired at 2130°C, 2.2 MPa, 30 minutes in the first step and 1985°C, 3.5 MPa, 30 minutes in the second step. After firing, the Si_3N_4 powder which was painted on was white in color as was the surface of the specimen, which was distorted due to differential shrinkage.

A BN crucible (6.5 cm dia. x 2.5 cm high was machined and was heat treated to remove impurities. The crucible was loaded with loose SN502 Si_3N_4 powder several times and heated to 2200°C under 320 psi N_2 in order to "season" the crucible. Subsequent firings of test bars revealed that BN transport remained as a problem. The only way found to date to minimize BN transport is to load the crucible with as many samples as possible to provide a small ratio of crucible volume/sample volume and/or crucible surface/sample surface.

The use of a graphite crucible proved to be unsuccessful since the Si_3N_4 sample was partially converted to SiC. Also, the use of a SiC setter during firing was unsuccessful as evidenced by "dishing" of the sample.

V. MECHANICAL PROPERTIES

A. Modulus of Rupture

1. Qualification of Scaled-up Material

Initial M.O.R. measurements were made to qualify the success of the scale-up procedures. Five bars were prepared from Batch SN502-95 containing 7 w/o $BeSiN_2$ with an oxygen content of $\sim$3.6 w/o. The specimens were fired in 3 separate runs with nearly identical firing schedules which included a 20 minute isothermal hold at 2115°C at 2.2 MPa N_2 pressure in the first step and 1990°C, 6.9 MPa for 25 minutes in the second step. The final densities of the 5 specimens were 99.2%, 99.2%, 99.4%, 99.1% and 99.1%, thus indicating reproducible densification for a given firing schedule. The length of each sintered bar was approximately 4.5 cm. Three-point bend specimens were prepared by surface grinding the samples with a 320 grit wheel at 0.0005" per pass until the faces were flat and parallel. Then 0.002" were removed from each face of the bar with a 500 grit wheel at 0.0002" per pass. Finally the edges were hand chamfered with a 15 μm diamond lap. The modulus of rupture was determined by 3-point bending with a span length of 3.8 cm and a crosshead speed of 0.5 mm/min. The results are presented in Table VIII.

Table VIII

M.O.R. Results of Scaled Up GPS Si_3N_4

Sample #	$\% \rho_{th}$	W (cm)	h (cm)	l (cm)	M.O.R.(MNm^{-2})
1	99.2	0.60	0.61	3.81	522
2	99.2	0.62	0.62	3.81	416
3	99.4	0.62	0.62	3.81	476
4	99.1	0.55	0.55	3.81	349
5	99.1	0.55	0.55	3.81	431

The average M.O.R. was 439 MNm^{-2} (63,668 psi) with a standard deviation of 65 MNm^{-2} and a Weibull modulus of 7.8. Results obtained in the previous contract (EC-76-A-1017-002) are summarized in Table XI.

Table XI

Summary of Previous Results

Billet #	M.O.R. MNm^{-2}	Weibull Modulus	# Specimens
35 & 38	560	9.1	8
77	597	8.3	5
78	496	8.7	5

The results summarized above were obtained from specimens fired in the small high N_2 pressure furnace and represent a sample size of 0.25 cm x 0.25 cm x 1.9 cm (span) or a volume of 0.12 cm^3. The average M.O.R and Weibull modulus of all samples are 551 MNm^{-2} and 8.7 respectively. It is possible to calculate if the lower strength obtained from the larger samples (0.58 x 0.58 x 3.81 cm) is consistent with the Weibull concept.

The average modulus of rupture of a group of specimens represents the strength at which there is 50% probability of failure. By assuming an average value of m and equating the probability of failure for the large volume and small volume samples sets, it is possible to predict the average strength of

any given sample volume. It will also be assumed that the strength-limiting flaw distribution exists within the volume of the material rather than at the surface. The probability of failure (P) for this case is:

$$P = 1 - e^{-KV\left(\frac{\sigma}{\sigma_o}\right)^m}$$

where P = probability of failure

K = geometrical constant, for 3 pt. bend $K = \frac{1}{2(m+1)^2}$

m = Weibull Modulus

V = sample volume

σ = average 3-point bend strength

σ_o = Normalizing Weibull parameter

By equating the probability of failure for the larger (P_L) and small volume (P_S) sample sets one obtains:

$$P_L = P_S$$

$$1 - e^{-KV_L\left(\frac{\sigma_L}{\sigma_o}\right)^m} = 1 - e^{-KV_S\left(\frac{\sigma_S}{\sigma_o}\right)^m}$$

$$\frac{V_L}{V_S} = \left(\frac{\sigma_S}{\sigma_L}\right)^m$$

$$\ln \frac{V_L}{V_S} = m \ln\left(\frac{\sigma_S}{\sigma_L}\right)$$

where: $V_S = 0.25 \times 0.25 \times 1.91 = 0.12\ cm^3$

$V_L = 0.58 \times 0.58 \times 3.81 = 1.28\ cm^3$

$\sigma_S = 551\ MNm^{-2}$

$m = 8.7$

$$\ln \frac{1.28}{0.12} = 8.7 \ln \frac{551}{\sigma_L}$$

$$\sigma_L = 420\ MNm^{-2}$$

Therefore, the predicted M.O.R. for the larger volume samples is 420 MNm^{-2}. The actual M.O.R. was 439 MNm^{-2} which is within 5% of the predicted value, thus giving good agreement. The Weibull modulus was estimated from a sample size of 18 specimens which can lead to an uncertainty of $\pm$30% in the actual value of m with an 80% confidence bound[21]. The plotted Weibull modulus, m, for the large specimens was 7.8.

2. Fracture Origins

All 5 M.O.R. specimens were examined by SEM after testing to determine the location of the fracture origins and the nature of the flaw at the origin. All fracture origins were observed to be in the volume of the material, not the surface. There were 2 apparent types of flaws: (1) porous regions and (2) inclusions. Figure 8a and b show an example of a porous region as the strength-limiting flaw. It was observed that the Si_3N_4 grains in the porous region are large and have a high aspect ratio. Figure 9 a and b show an example of an inclusion as the strength-limiting flaw. The chemical composition of the included phase was not identified.

3. Effect of Heat Treatment on the Room Temperature Modulus of Rupture

Twenty bars (5.8 cm x 0.8 cm x 0.8 cm before firing) were prepared from Batches SN502-87 (prepared under previous AMMRC contract) and SN502-100 containing 7 w/o $BeSiN_2$ with an oxygen content of 3.5 w/o. The specimens were fired with a 30 minute isothermal hold at 2105°C under 2.2 MPa N_2 pressure in the first step and a 30 minute isothermal hold at 1950°C under 6.9 MPa N_2 pressure in the second step. After sintering, the bars were machined as described previously and divided in four groups for heat treatment and M.O.R. testing. Group 1 was tested in the as-machined condition. Group 2 received a 1 hour treatment in air at 1300°C prior to

testing. Group 3 was annealed at 1600°C for 8 hours under 1.8 MPa of N_2 before testing. Group 4 was annealed at 1600°C for 8 hours under 1.8 MPa of N_2 followed by a 1 hour treatment in air at 1300°C prior to testing. Modulus of rupture measurements were determined by 3-point bending with a span length of 3.8 cm and a crosshead speed of 0.5 mm/min. The results are presented in Table X.

Table X

M.O.R. Results of Heat Treated GPS Si_3N_4

Group #	$\%\rho_{th}$	h (cm)	w (cm)	l (cm)	M.O.R. (MPa)
1	99.3	0.52	0.61	3.81	447
	99.2	0.52	0.61	3.81	367
	99.2	0.52	0.61	3.81	386
	99.2	0.52	0.61	3.81	395
	99.2	0.52	0.52	3.81	405
2	99.8	0.52	0.62	3.81	412
	99.0	0.52	0.62	3.81	482
	NA	0.52	0.62	3.81	415
	99.0	0.52	0.52	3.81	379
	99.5	0.51	0.62	3.81	381
3	99.7	0.52	0.62	3.81	391
	99.6	0.51	0.62	3.81	469
	NA	0.48	0.62	3.81	319
	NA	0.48	0.62	3.81	476
	99.4	0.51	0.62	3.81	445
4	NA	0.52	0.62	3.81	548
	98.9	0.52	0.62	3.81	402
	99.4	0.52	0.62	3.81	476
	99.5	0.50	0.62	3.81	644
	99.5	0.51	0.62	3.81	412

After M.O.R. testing the data was analyzed for average strength, standard deviation and Weibull Modulus. The results of the analysis are presented in Table XI.

Table XI

Results of Heat Treated M.O.R. Specimens

Group #	Ave. M.O.R. (MPa)	Std. Deviation (MPa)	Weibull Modulus
1	400.0	29.5	15.3
2	414.7	41.7	10.8
3	419.9	65.5	6.9
4	496.1	101.0	5.6

The results show that all heat treatments increase the average M.O.R. of GPS Si_3N_4. Group #4, which was annealed at 1600°C for 8 hrs in N_2 and oxidized for 1 hr in air at 1300°C, had the highest average value of 496 MPa. It must be recognized that only a small number of specimens (5) were broken for each treatment and the accuracy of the statistics is questionable. For a sampling size of 5, the real Weibull Modulus, m, could be 40% lower or 80% higher with an 80% confidence bound[21].

4. High Temperature Modulus of Rupture

Test bars from scaled-up GPS Si_3N_4 were machined by the procedure described previously to provide specimens of dimensions of $\sim$0.25 cm x 0.50 cm x 3.8 cm. The specimens were broken in 3-point bending in air at 1400°C and 1500°C. The results are presented in Table XII.

Table XII

High Temperature M.O.R. of Scaled-Up GPS Si_3N_4

Test Temperature °C	h (cm)	w (cm)	l (cm)	M.O.R. (MPa)
1400	0.27	0.50	3.81	377
1400	0.27	0.50	3.81	409
1400	0.27	0.50	3.81	445
1500	0.27	0.50	3.81	232
1500	0.27	0.50	3.81	292
1500	0.27	0.50	3.81	313

Analysis of the test results showed that at 1400°C the average strength was 410 MPa with a standard deviation of 34 MPa and a Weibull Modulus of 13.8. At 1500°C the average strength was 279 MPa with a standard deviation of 42 MPa and a Weibull modulus of 7.2. Again the number of samples tested was small and the values of the Weibull Modulus are certainly questionable, however the values of the average strength should be quite representative.

Figure 10 presents a plot of M.O.R. vs. temperature and shows excellent strength retention at 1400°C, and a sharp decrease in strength between 1400°C and 1500°C. The 2 curves shown in Figure 10 represent the average M.O.R. vs. temperature for different sample sizes. Examination of the fracture origins in GPS Si_3N_4 has revealed that the strength-limiting flaws are porous regions which exist in the volume of the test bar rather than machining or surface flaws. The upper curve represents the M.O.R. vs. temperature for test bars with a sample size of 0.25 cm x 0.25 cm x 1.9 cm (span) or a volume of 0.12 cm^3. The room temperature data point of 551 MPa was determined from the 18 test specimens broken under the previous AMMRC contract (#EC-76-A-1017-002). The data points at 1400°C and 1500°C were obtained by taking the data presented in Table XII and scaling it to the small sample size (0.12 cm^3) by the procedure previously described which assumed m = 8.7. The room temperature data point in the lower curve was taken from the 10 bars (0.58 x 0.58 x 3.81 cm) which were broken in the as-machined condition (See Table VIII and Table X). Combining these 2 sets of test bars yielded an average strength of 420 MPa, a standard deviation of 52 MPa and a Weibull Modulus of 9.7. The data points at 1400°C and 1500°C were obtained by taking the data presented in Table XII and scaling it to the large sample size (1.25 cm^3) by the procedure previously described which assumed m = 8.7.

5. Fracture Origins

Fracture origins of the highest and lowest strength bars for each of Groups 1 - 4 were identified by scanning electron microscopy of the fracture surfaces. The predominant strength-limiting flaw was found to be porous regions in the bulk of the specimen. The origin of the porous regions is unclear at this point. One possibility is a non-uniform distribution of $BeSiN_2$ densification aid. It is believed, however, that this is not the probable cause since at the sintering temperature the liquid is highly reactive and should wet all grain surfaces. A more probable cause may be the presence of hard agglomerates after drying of the milled, leached and washed powder which are never broken up during mixing of the lubricant in the mortar and pestle or during pressing. Further gains in strength may be possible with improved procedures for preparing green compacts.

B. Creep

The creep behavior of GPS Si_3N_4 was measured in air as a function of temperature at a constant stress of 207 MPa (30,000 psi). Creep determination was made on a test bar machined from sample SN502-95-9 which produced 3 creep specimens. The creep specimen (2.5 mm x 2.5 mm x 4.5 cm) was loaded in a 3-pt. bending mode using SiC fixtures with a span of 2.24 cm. Deflection of the test specimen was measured with a DC-operated LVDT manufactured by Schaevity Engineering, Model #050DC-D and had a sensitivity of 80 V/cm.

It was found that the placement of the core inside the LVDT was not in the calibrated portion of the detector. However, the voltage versus displacement of the LVDT was determined for the arrangement used during the creep runs. It was found that the sensitivity of the LVDT was 12.47 volts/cm. Although some error may be possible, the results are believed to be accurate to within 20%.

The furnace was heated to 1300°C and allowed to equilibrate for 5 hrs. prior to applying the stress of 207 MPa (30,000 psi) which was accomplished by dead weight loading external to the furnace. The stress was applied for a period of 23 hrs. and a power outage caused a shut down of the creep rig. The load was again applied and allowed to creep for 23 hrs. in order to reach steady state creep. Measurement of creep rate at 1300°C under 207 MPa was then measured over a 92 hr. period. Using a stress exponent, n, of 2.2 the calculated steady state strain rate, $\dot{\varepsilon}$, was 7.9 x 10^{-7}/hr. With the load applied the furnace temperature was then raised to 1400°C and the sample allowed to creep for 27 h to attain steady state. Measurement of creep rate at 1400°C was done over a 45 hr. period and was calculated to be 3.2 x 10^{-6}/hr assuming n=2.2. The temperature was dropped to 1350°C and allowed to equilibrate under load for 32 hrs. Measurement of creep rate at 1350°C was done over a 174 hr. period and was calculated to be 5.76 x 10^{-7}/hr. The thermocouple on the creep rig failed causing the furnace to shut down. The furnace was cycled from room temperature to 1300°C three times during repairs. The creep rate at 1300°C was measured again over a 115 hr period and was calculated to be 3.90 x 10^{-7}/hr. assuming n=2.2. This creep rate was a factor of 2 lower than the first measurement at 1300°C. This effect may be associated with the "annealing" effect previously reported by Greskovich and Palm[18] (Final Rept. Contract #DAAG46-78-C-0058).

A second creep specimen (SN502-95-9-2) was tested in the same sequence as reported above, namely, at 1300°C, 1400°C, 1350°C and 1300°C under a stress of 207 MPa (30,000 psi). Very good agreement was observed between the 2 specimens, and the results presented in Figure 11 show the creep rate as a function of temperature for GPS Si_3N_4 under a stress of 69 MPa and 210 MPa. The results show that the creep rate of the GPS Si_3N_4 is

probably dependent in a favorable way on thermal history which is consistent with the "annealing" effect reported by Greskovich and Palm.

The creep specimen (SN502-95-9-2) was heated to 1300°C in 3 hrs and allowed to equilibrate for 16 hrs with only the weight of the load train applied (0.5 MPa (3700 psi)). The load was applied to give a stress of 207 MPa (30,000 psi), and the specimen was allowed 30 hrs. to attain steady state creep before the measurement was initiated. The creep rate at 1300°C under 207 MPa was measured over a 67 hr. period and was found to be 5.27×10^{-6} /hr assuming a stress exponent, n, of 2.2. With the load applied the furnace was raised to 1400°C and allowed to creep for 15 hrs to attain state. Measurement of creep rate at 1400°C was done over a 36 hr period and found to be 3.75×10^{-5}/hr assuming n = 2.2. The temperature was dropped to 1350°C and allowed to equilibrate under load for 36 hrs. The creep rate at 1350°C was measured over a 55 hr. period and was found to be 4.45×10^{-6}/hr. The furnace was then dropped to 1300°C and the creep rate measured again over a 28 hr. period and was found to be 2.62×10^{-6}/hr.

The above sequence of testing allowed the specimen to be stressed at 207 MPa (30,000 psi) for 125 hrs. at 1300°C, 91 hrs. at 1350°C and 51 hrs. at 1400°C. Maintaining the temperature at 1300°C, the load was increased to 345 MPa (50,000 psi). The specimen was then held at 1300°C for 650 hrs. with a 345 MPa (50,000 psi) stress without sample failure, a result not previously demonstrated. The measured creep rate was observed to decrease with time and the results are shown in Table XIII which presents the observed creep rate, $\dot{\varepsilon}$, over various time intervals. A major conclusion from these results is the very low creep rates observed for GPS Si_3N_4 at 1300°C in air when 50,000 psi (maximum tensile stress) is applied for 650 h. In addition, the sample showed little total creep strain and little difference in appearance from an as-machined test bar.

Table XIII

Observed Creep Rate versus Time at 1300°C Under 345 MPa Stress

Time Interval (hrs)	$\dot{\varepsilon}$ (hr^{-1})
0 - 50	4.09×10^{-6}
50 - 100	3.07×10^{-6}
100 - 200	2.22×10^{-6}
200 - 300	1.36×10^{-6}
300 - 400	1.02×10^{-6}
400 - 500	1.71×10^{-6}
500 - 600	6.82×10^{-7}
600 - 650	6.82×10^{-7}

VI. OXIDATION RESULTS ON GPS Si_3N_4

The oxidation behavior of dense (>99%), GPS Si_3N_4 was investigated over the temperature range of 1000 to about 1400°C in oxygen for times up to 500 h. Typically, bar-shaped samples were used that had surface areas betwen 5 and 12 cm^2 and weights between 1 and 5 grams.

The oxidation of clean test pieces of sintered Si_3N_4 finished with 500 grit diamond was accomplished in a Al_2O_3 tube furnace. Bars were leached in concentrated HCl for 2 h. and then washed in distilled water and in alcohol, respectively. A specimen was placed on an oxidized SiC setter which lay on a Al_2O_3 boat and inserted into the hot furnace within 5 minutes. During the oxidation experiment, the furnace temperature was controlled within $\pm$ 2°C. The specimen was periodically removed from the hot furnace and its weight measured on a Mettler H54 AR balance capable of measuring to the nearest 2×10^{-5}g. The amount of oxidation was determined from weight gain measurements expected according to the reaction $Si_3N_4 + 3\ O_{2(g)} \rightarrow 3\ SiO_2 + 2\ N_{2(g)}$. Parabolic oxidation kinetics were observed in all cases and the parabolic rate constant (k_p) was determined by using equation,

$$(\Delta W/A)^2 = k_p t,$$

where W/A is the change in weight per unit area and t is the oxidation time.

The oxidation results for GPS SI_3N_4 oxidized at 1300, 1355 and 1405°C are shown in Fig 12. Here, the data is presented on a $(\Delta W/A)^2$ versus t plot for which a linear curve indicates parabolic oxidation kinetics. The general, overall oxidation data show that the GPS Si_3N_4 composition exhibits excellent oxidation resistance. For example, after 300 h. of oxidation at 1300°C the weight gain per unit area ($\Delta W/A$) was only $(0.8\ g^2m^{-4})^{\frac{1}{2}}$ or less than 0.1 mg/cm^2. The $\Delta W/A$-value was only $(\sim 2.2\ g^2m^{-4})^{\frac{1}{2}}$ or $\sim$ 0.15 mg/cm^2 for oxidation at 1405°C for $\sim$ 300 h. The parabolic rate constants for oxidation at 1300, 1355 and 1405°C were 7.4×10^{-13}, 1.4×10^{-12} and 2.1×10^{-12} kg^2 m^{-4} s^{-1}, respectively. These results show that the scale-up GPS Si_3N_4 has an oxidation rate $\sim$ 2-3 orders of magnitude lower than that for commerically hot pressed NC-132 Si_3N_4 oxidized in the same furnace at 1400°C. The activation energy for oxidation was calculated from the slope of the plot of log k_p versus 1/T for the three data points and was determined to be 209 kJ/mole (50 kcal/mole). This activation energy is only about ½ the value previously determined on the "same" GE composition that was probably oxidized under "contaminated" conditions[18].

A long term oxidation experiment carried out at 1300°C for 500 h showed that the sample still followed parabolic behavior and showed little color change as compared to the unoxidized material. The $\Delta W/A$-value for this sample was found to be 0.12 mg/cm^2, a very low value for Si_3N_4 ceramics. A 100 h exposure at 1000°C in flowing oxygen also showed no detectable weight gain or no measureable oxidation.

The oxidized samples were characterized by XRD analysis and optical microscopy. The x-ray spectra of various samples oxidized at 1300-1400°C showed only the presence of -cristobalite in the oxide scale. Optical microscopy and

visual inspection showed a fine network of microcracks in the oxide film which was very thin and coherently-bonded to the Si_3N_4 substrate.

VIII. DETERMINATION OF POSSIBLE BERYLLIUM LOSS FROM GPS Si_3N_4

A small gas burner rig was designed and constructed to determine if there was any Be loss from the sintered Si_3N_4 under oxidizing conditions at 1200°C. The gas burner rig, shown schematically in Figure 13, provided an enclosed reaction chamber whose components, which were down stream from the Si_3N_4 samples, were sulphuric acid-leached after the experiment to determine if a Be loss occurs. Since the atmosphere in the reaction chamber is oxidizing, it was anticipated that the Be should exist as BeO or a Be-containing oxide or hydroxide which is soluble in H_2SO_4. The reaction tube was heated by a Kanthal A-1 wound tube furnace that was fitted with microprocessor programming and proportional band control. The control thermocouple (Pt-Pt/10% Rh) was placed between the I.D. of the wound tube and the O.D. of the reaction tube to provide for minimum temperature fluctuation in the reaction tube. An additional Type S thermocouple was placed inside the reaction tube to monitor the sample temperature. The torch gas and air flows were monitored by flowmeters as was the excess air flow. The air to fuel ratio was 7.5/1, or 9 standard CFH of air and 1.3 standard CFH of city gas. The torch was adjusted so that the flame directly impinged on the samples. The hot gas passed over the sample and through a bed of pyrex beads which were held in place on either end by porous alumina plugs. Water cooling coils provided a heat sink so that gas passing through the bubbler was not hot. At the gas flows utilized, about 35 ml/hr of H_2O were produced, thus making it necessary to remove water from the bubbler periodically. The water which was periodically removed was evaporated, and the residue was analyzed for Be.

The gas burner rig test was conducted for 525 hours at 1200°C to determine the possible loss of beryllium from dense (> 99%) GPS Si_3N_4. The Si_3N_4 used in the experiment had an initial weight of 11.65 grams and a surface area of 58 cm^2.

After testing the GPS Si_3N_4 appeared to still have sharp edges and corners, suggesting little material erosion under test conditions. During this long term experiment the GPS Si_3N_4 exhibited a weight gain of 0.07 w/o caused by possibly both oxidation and/or impurity pick-up from the gas or the mullite furnace tube. It was noted that some of the surfaces of the GPS Si_3N_4 had a very shiny, smooth, glass-like appearance after the gas burner test. Energy dispersive analysis (EDA) by X-ray and XRD were conducted to determine what cation impurities and phases were present as compared to the surfaces of the GPS Si_3N_4 not exhibiting the shiny surface layer. The XRD results showed no difference and the phases present were β-Si_3N_4 and α-cristobalite. E.D.A. results showed the presence of K and Ti impurities on the sample having the shiny surface. The McDanel MV30 mullite tube is reported to contain 0.5 w/o TiO_2 and 0.7 wt% K_2O and is therefore the source of the impurities found.

The total internal surfaces of the burner rig system were washed (leached) with surfuric acid to dissolve any existing BeO, Be-containing oxide or hydroxide that might have escaped as airborne species from the GPS Si_3N_4 ceramic. Leaching was done in the same glass tray that was used for evaporation of the water which was removed from the bubbler. This insured that all Be would be collected. The acid solution was then evaporated and the residue collected. A sample of the residue was analyzed for Be by atomic absorption spectroscopy and was found to contain 0.16 w/o in the residue. The residue collected weighed 0.74 g and corresponds to a total weight loss of 1.2×10^{-3} g of Be from 11.659 g of GPS Si_3N_4, corresponding to a 0.01% weight loss. By considering the amount of air (8.0 cfh) and gas (2.5 cfh) flowing through the gas burner rig, it was calculated that the exit gas contained 6 ppb by weight of beryllium.

It is speculated that the Be is removed from the GPS Si_3N_4 as $Be(OH)_2$. More experiments will have to be conducted to determine if the only Be removed is

that which is contained in the oxidized layer on the surface of the GPS Si_3N_4 or if Be will continually diffuse from the bulk and through the SiO_2 layer.

IX. ADDITIONAL SINTERING STUDIES

1. Sintering of Starck LC-12

Initial sintering experiments have been conducted on Starck LC-12 Si_3N_4 with the addition of 7 w/o $BeSiN_2$. The $BeSiN_2$ was added to the LC-12 powder by wet mixing in a nalgene jar with heptane and Si_3N_4 media on a paint shaker for one hour. One gram cylindrical specimens (1.0 cm dia x 1 cm high) were cold pressed at 3200 psi and isopressed at 30,000 psi. These specimens were then oxidized to yield a total oxygen content of 2.45 w/o, 3.22 w/o and 3.44 w/o. All specimens were fired at 2110°C for 30 minutes under 330 psi N_2 pressure in the first step and 1950°C for 30 minutes under 1000 psi N_2 pressure. The specimen containing 2.45 w/o oxygen achieved a final density of 98.5%. Sectioning after firing revealed the presence of a crack at the center of the specimen. The cause of this crack is unknown at this time. It should also be noted that a lower oxygen content is required to achieve high density for the LC-12 powder compared to the SN-502 powder. The specimens containing 3.22 w/o and 3.44 w/o oxygen achieved fired densities of 94.3% and 94.2% respectively. Sectioning after firing revealed that gross bloating had occurred. Again, the cause of the bloating is not understood. It is apparent, however, that both the firing schedule and the oxygen content will have to be optimized specifically for the LC-12 powder.

2. Sintering of Si_3N_4 Containing 7 w/o $BeSiN_2$ Which Was Injection Molded by AiResearch

A batch of $BeSiN_2$ (150 g) was prepared and shipped to Karsten Styhr at AiResearch. Using their own procedures, the $BeSiN_2$ was added to SN502 Si_3N_4 and injection molded. Four injection molded test bars with the binder

removed were received. The bars were placed in a furnace and heated slowly (400°C/hr) to 600°C for ∿ 90 minutes in air to insure complete binder removal. A weight loss of 1.2% was observed and 2 of the bars had cracks in them indicating that the heating rate was probably too high. The green density of the injection molded bars were measured to be 58.8% which is quite high relative to the 52.7% observed for the pressing procedure used at GE. It was determined that oxidation at 920°C for 30 minutes in air gave an oxygen content of 3.9 w/o. Two bars were required for determination of the oxidation conditions and the other 2 were sintered. Sintering conditions were a 30 minute isothermal hold at 2110°C under 2.2 MPa N_2 pressure in the first step and a 30 minute hold at 1950°C under 6.9 MPa N_2 in the second step. Final densities were 98.0% and 97.8% of theoretical. After firing, the bars exhibited some bloating, indicating that most of the sample had achieved full density.

Six more bars were received from K. Styhr so that the bloating problem could be eliminated. The previously dewaxed test bars were heated to 650°C for 45 minutes in air and a 0.75% weight loss was observed. Bar #11 was oxidized at 885°C for 30 minutes to yield O_T = 3.8. Sintering at 2110°C for 30 minutes under 2.2 MPa N_2 in the first step and 1950°C for 30 minutes under 6.9 MPa N_2 in the second step yielded a density of 97.9% and a weight loss of 2.1 w/o. Bloating of the sample was still apparent. Bar #12 was oxidized at 850°C for 30 minutes in air to yield O_T = 3.1 w/o. Sintering was done by dropping the temperature in the 1st step by 100°C to 2010°C with all other conditions kept the same as previous firings. The specimen achieved 100% density and a weight loss of 0.5 w/o. Bars #13 - 19 were the oxidized at 855°C for 30 minutes in air and yielded O_T = 3.3 w/o. Table XIV summarizes the densities and weight losses observed after sintering at 2010°C for 30

minutes under 2.2 MPa in the first step and 1950°C for 30 minutes under 6.9 MPa in the second step.

Table XIV

Sintering Results of Injection Molded AiResearch Bars

Bar #	$\%\rho_f$	$\%\Delta W/W_f$
13	99.92	1.10
14	99.92	0.89
15	99.99	1.11
16	99.5	0.94
18	99.99	1.10
19	99.99	1.11

REFERENCES

1. A.E. Gorum, J.J. Burke, E.M. Lenoe, and R.N. Katz, in Proceedings of the NATO-CCMS Symposium on Low Pollution Power Systems Development, Dusseldorf, November 1974.
2. S. Prochazka, in Ceramics for High Performance Applications, edit, by J.J. Burke, A.E. Gorum and R.N. Katz, Brook Hill Pub. Co., Chestnut Hill, Mass., 1974.
3. G.R. Terwilliger, J. Am. Ceram. Soc. 57 48 (1974).
4. L. Pauling, The Nature of the Chemical Bond, Cornell Univ. Press. 1939.
5. K. Kijima and S. Shirasaki, "Nitrogen Self-Diffusion in Si_3N_4", J. Chem. Phys. 65 (7) 2668-71 (1976).
6. S. Wild, P. Grieveson, K.H. Jack and M.J. Latimer; pp. 377-84 in Special Ceramics 5. Edited by P. Popper. British Ceramic Research Association, Stoke-on-Trent, 1972.
7. R.R. Wills, "Silicon Yttrium Oxynitrides", J. Am. Ceram. Soc. 57 (10) 459 (1974).
8. L.J. Bowen, R.J. Weston, T.G. Carruthers and R.J. Brook, "Hot Pressing and the - Phase Transformation in Si_3N_4", J. Mat. Sci., 13 341-50 (1978).
9. C. Greskovich, "Hot-Pressed $-Si_3N_4$ Containing Small Amounts of Be and O in Solid Solutions" J. Mat. Sci. 14 2427-38 (1979).
10. F.F. Lange, "High Temperature Strength Behavior of Hot-Pressed Si_3N_4: Evidence For Subcritical Crack Growth", J. Am. Ceram. Soc. 57 (2) 84-87 (1974).
11. R. Kossowsky, D.G. Miller and E.S. Diaz, "Tensile and Creep Strengths of Hot-Pressed Si_3N_4", J. Mat. Sci. 10 983-97 (1975).
12. S.U. Din and P.S. Nicholson, "Creep of Hot Pressed Si_3N_4", ibid 10 1375-80 (1975).

13. B.S.B. Karunaratne and M.H. Lewis, "High-Temperature Fracture and Diffusional Deformation Mechanisms in Si-Al-O-N Ceramics", ibid 15 449-62 (1980).

14. G.R. Terwilliger and F.F. Lange, "Pressureless Sintering of Silicon Nitride, ibid 10 1169-74 (1975).

15. M. Mitomo, "Pressure Sintering of Si_3N_4", ibid 11 1103-07 (1976).

16. S. Prochazka and C. Greskovich, "Effect of Some Impurities on Sintering Si_3N_4", pps. 489-502 in Proc. of International Symposium on Factors in Densification and Sintering of Oxide and Non-oxide Ceramics, Edited by S. Somiya and S. Saito, Gakujutsu Bunken Fukyu-kai, Tokyo, Japan, 1978.

17. M. Mitomo, "The Sintering of Si_3N_4 Under High Nitrogen Pressures", ibid 539-544.

18. C. Greskovich and J.A. Palm, "Development of High Performance Sintered Si_3N_4", Final Technical Report, September 1980, Contract No. DAAG46-78-C-0058.

19. C. Greskovich and J.A. Palm, "Controlling the Oxygen Content of Si_3N_4 Powders", Am. Ceram. Soc. Bull. 59 (11) 1155-56 (1980).

20. I.C. Huseby, H.L. Lukas and G. Petzow, "Phase Equilibria in the System Si_3N_4-SiO_2-BeO-Be_3N_2", J. Am. Ceram. Soc. 58 (9-10) 377-80 (1975).

21. C.A. Johnson, "Confidence Bounds on Weibull Parameters", To be published by Am. Ceram. Soc.

Figure 1 SEM photomicrograph of a typical final processed powder. (10,000 X).

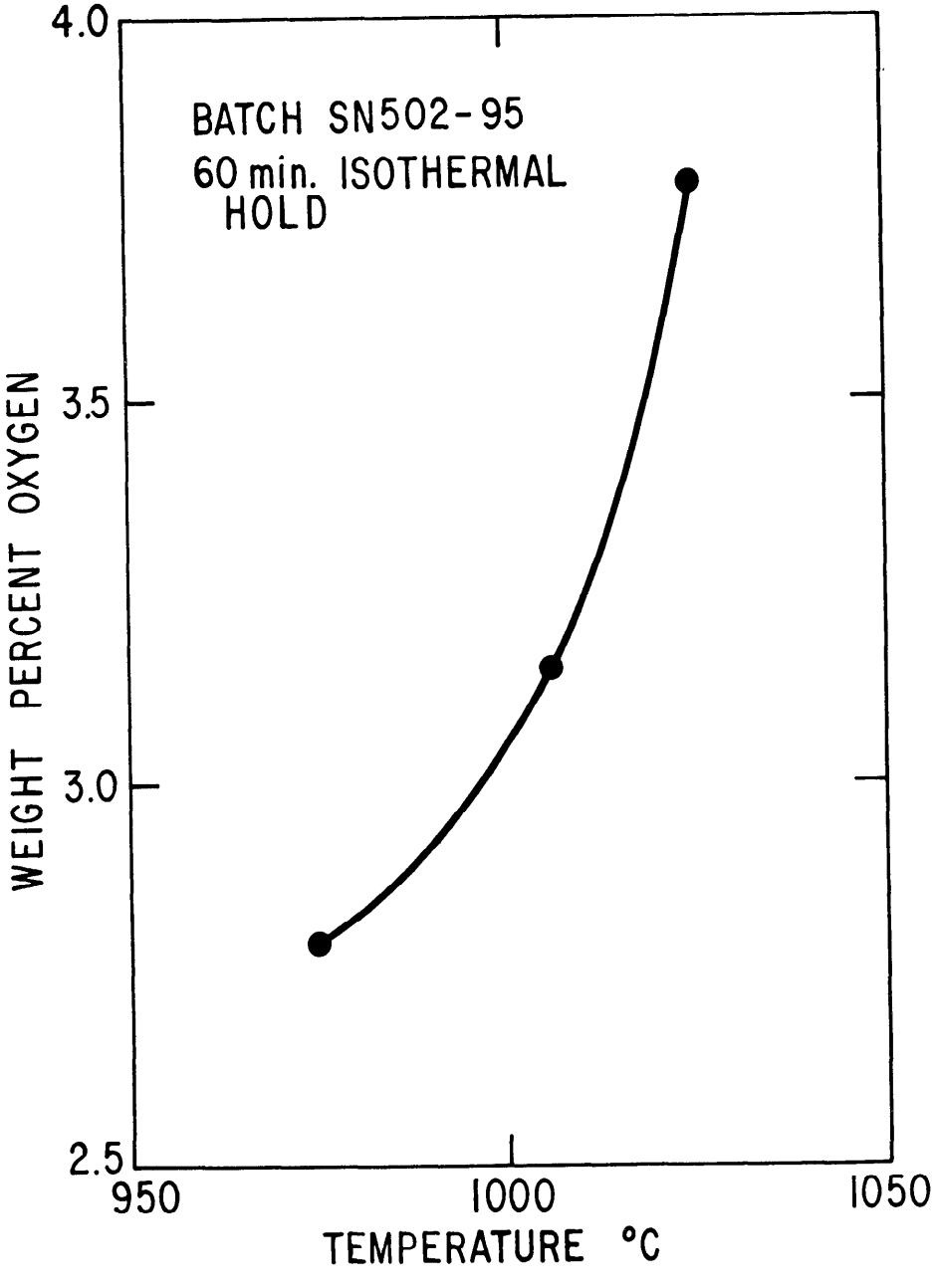

Figure 2 Oxidation behavior of compacts of SN502-95 as a function of temperature for a 60 minute isothermal hold.

Figure 3 SEM photomicrograph of sample SN502-95-12 which was fired at 2145°C under 2.2 MPa of N_2 for 30 minutes. (10,000 X).

Figure 4 SEM photomicrograph of sample SN502-95-13 which was fired at 2145°C under 2.2 MPa of N_2 for 60 minutes. (10,000 X).

Figure 5 SEM photomicrograph of sample SN502-95-14 which was fired at 2145°C under 2.2 MPa of N_2 for 30 minutes in the 1st step and 2045°C under 2.2 MPa of N_2 for 30 minutes in the 2nd step. (10,000 X).

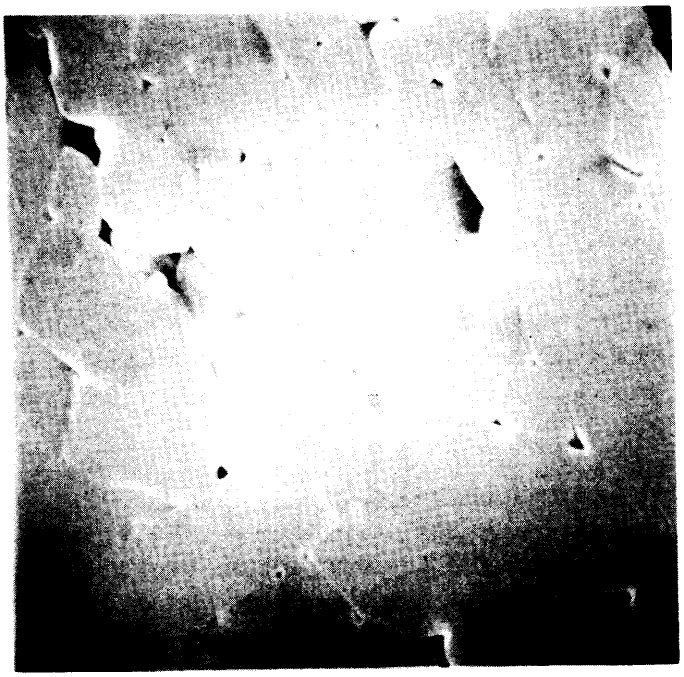

Figure 6 SEM photomicrograph of sample SN502-95-15 which was fired at 2145°C under 2.2 MPa of N_2 for 30 minutes in the 1st step and 2045°C under 2.2 MPa for 30 minutes in the 2nd step. (10,000 X).

Figure 7 SEM photomicrograph of sample SN502-95-16 which was fired at 2145°C under 2.2 MPa of N_2 for 30 minutes in the 1st step and 1945°C under 2.2 MPa of N_2 for 30 minutes in the 2nd step. (10,000 X).

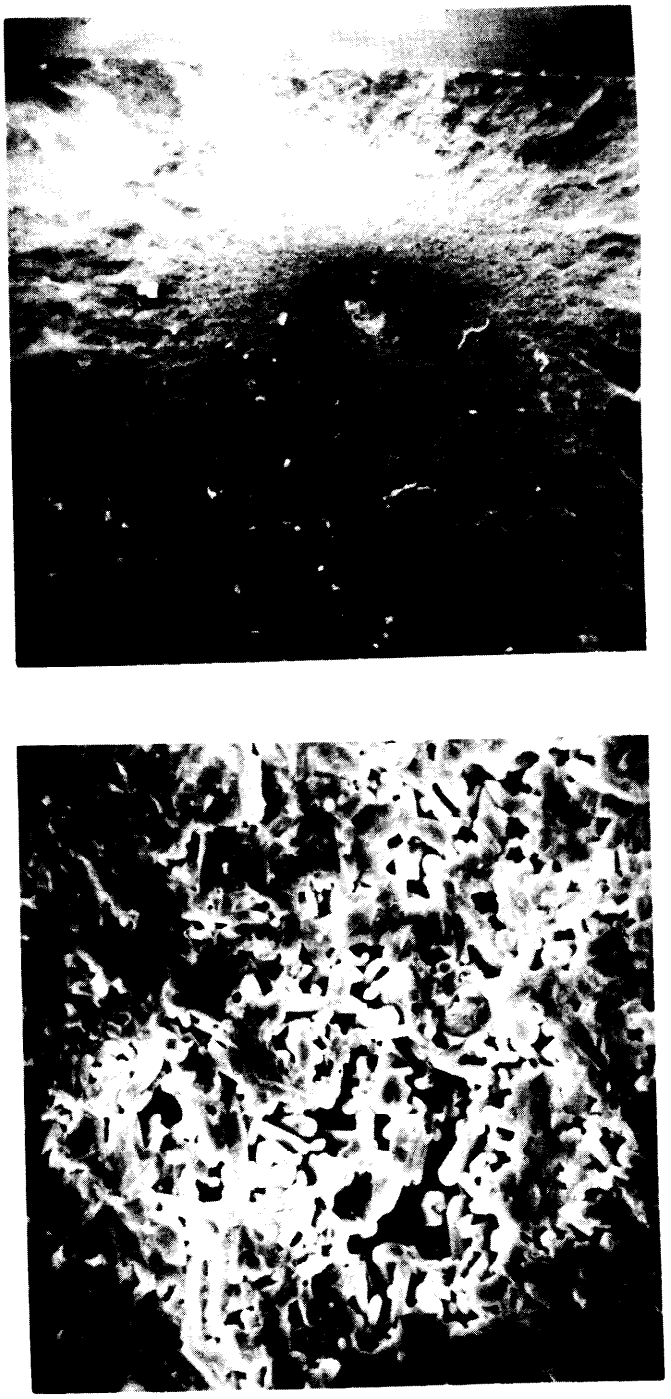

Figures 8a and 8b SEM photomicrograph showing an example of a porous region which is the strength limiting flaw at 60X and 1200X respectively.

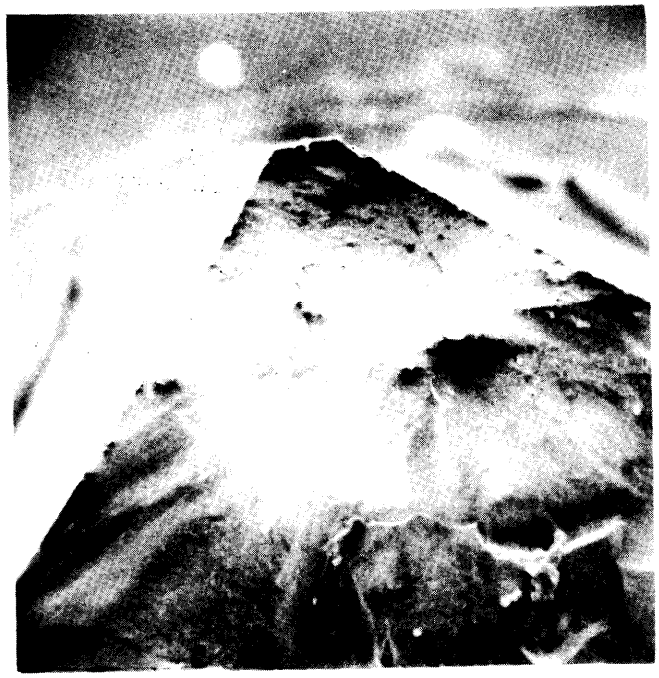

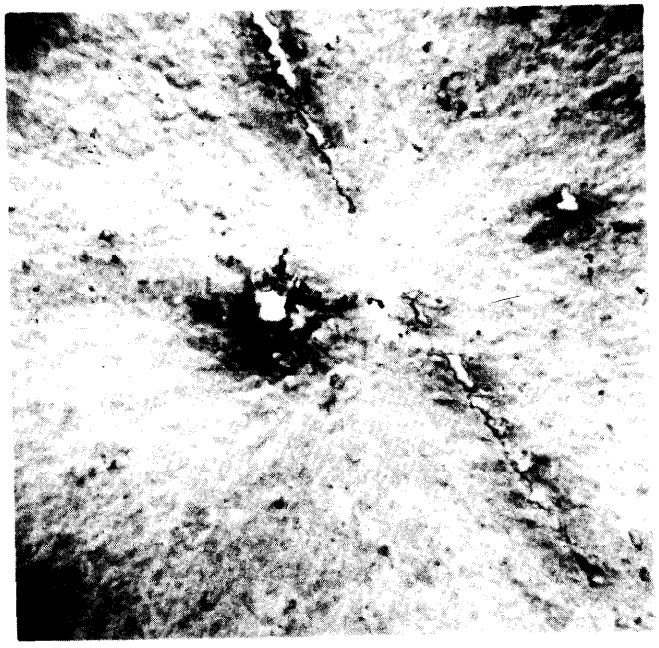

Figures 9a and 9b SEM photomicrograph showing an example of an inclusion which is the strength limiting flaw at 60X and 1200X respectively.

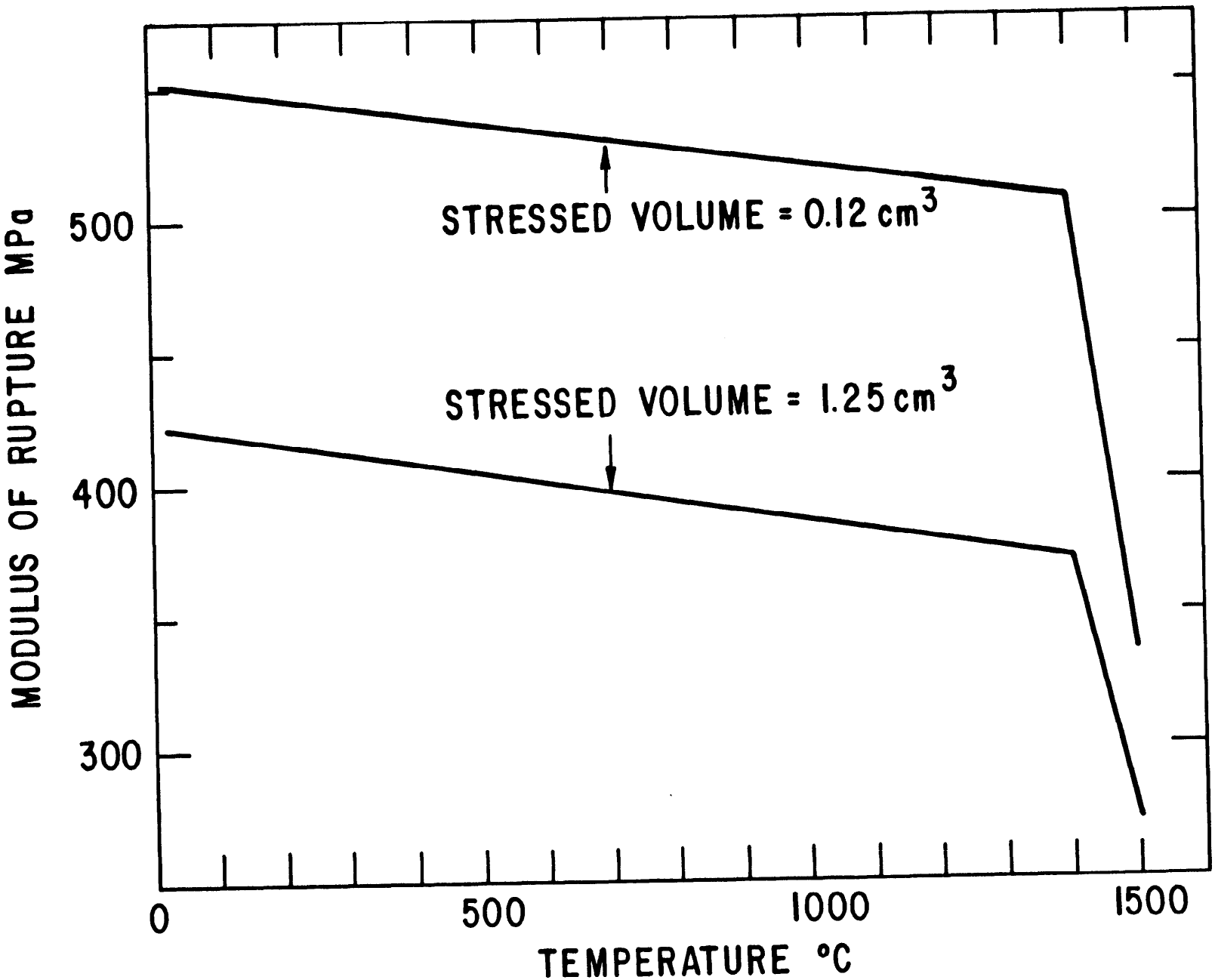

Figure 10 Modulus of rupture versus temperature for GPS Si_3N_4 scaled for a sample volume of 0.12 cm^3 and 1.25 cm^3 assuming m = 8.7.

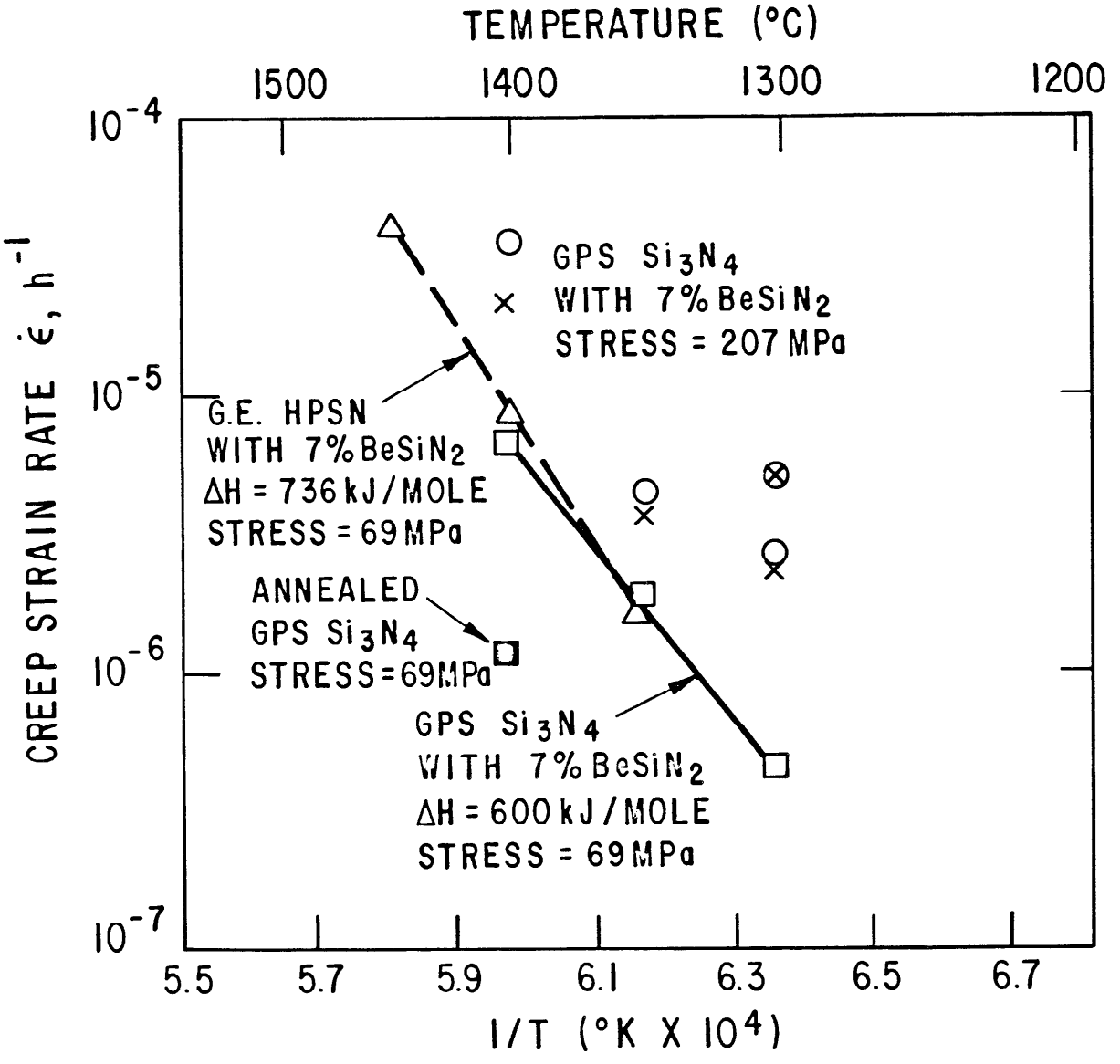

Figure 11 Steady state creep rate versus 1/T for GPS Si_3N_4.

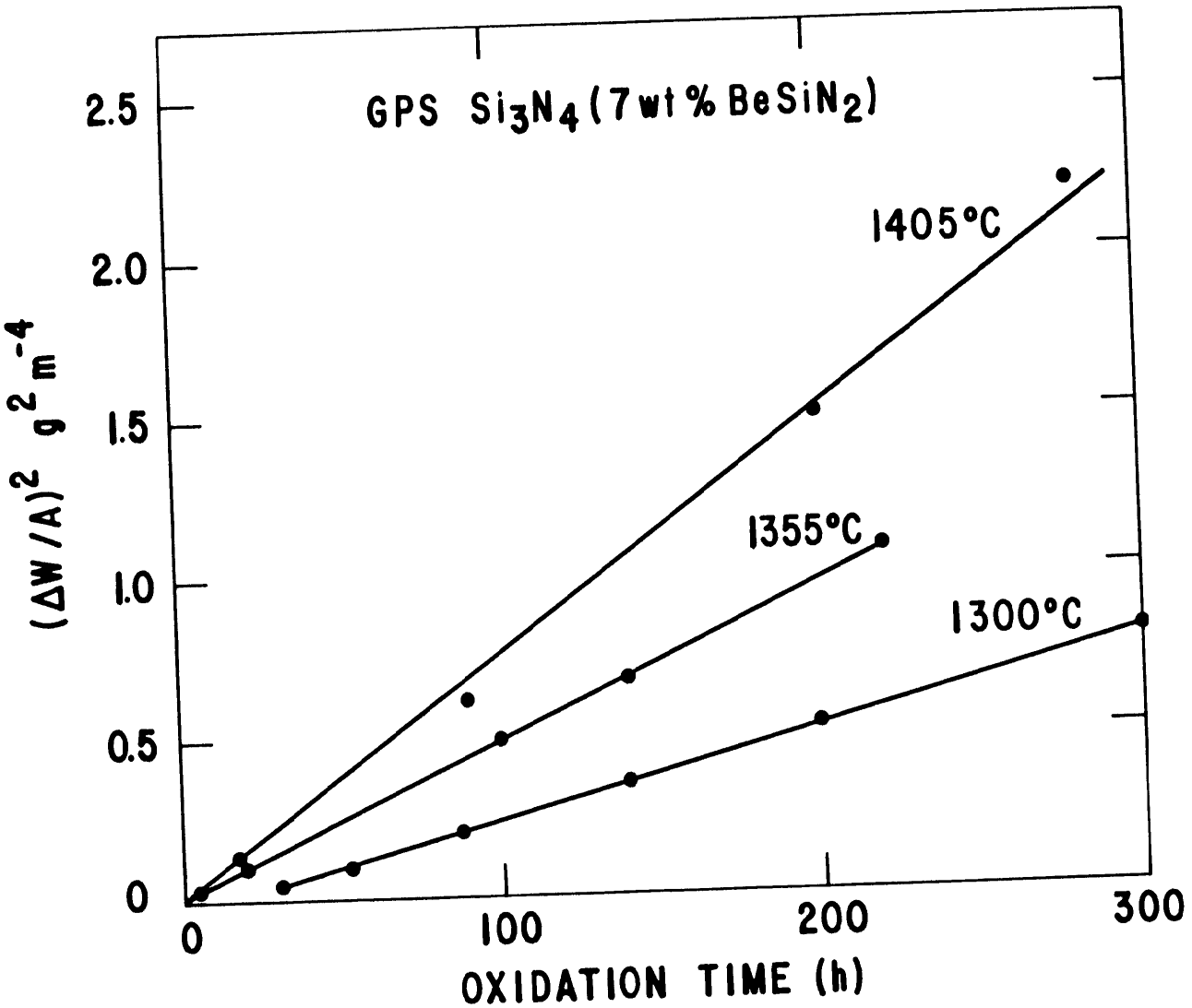

Figure 12 Oxidation kinetics of GPS Si_3N_4 at 1300°C, 1355°C and 1405°C.

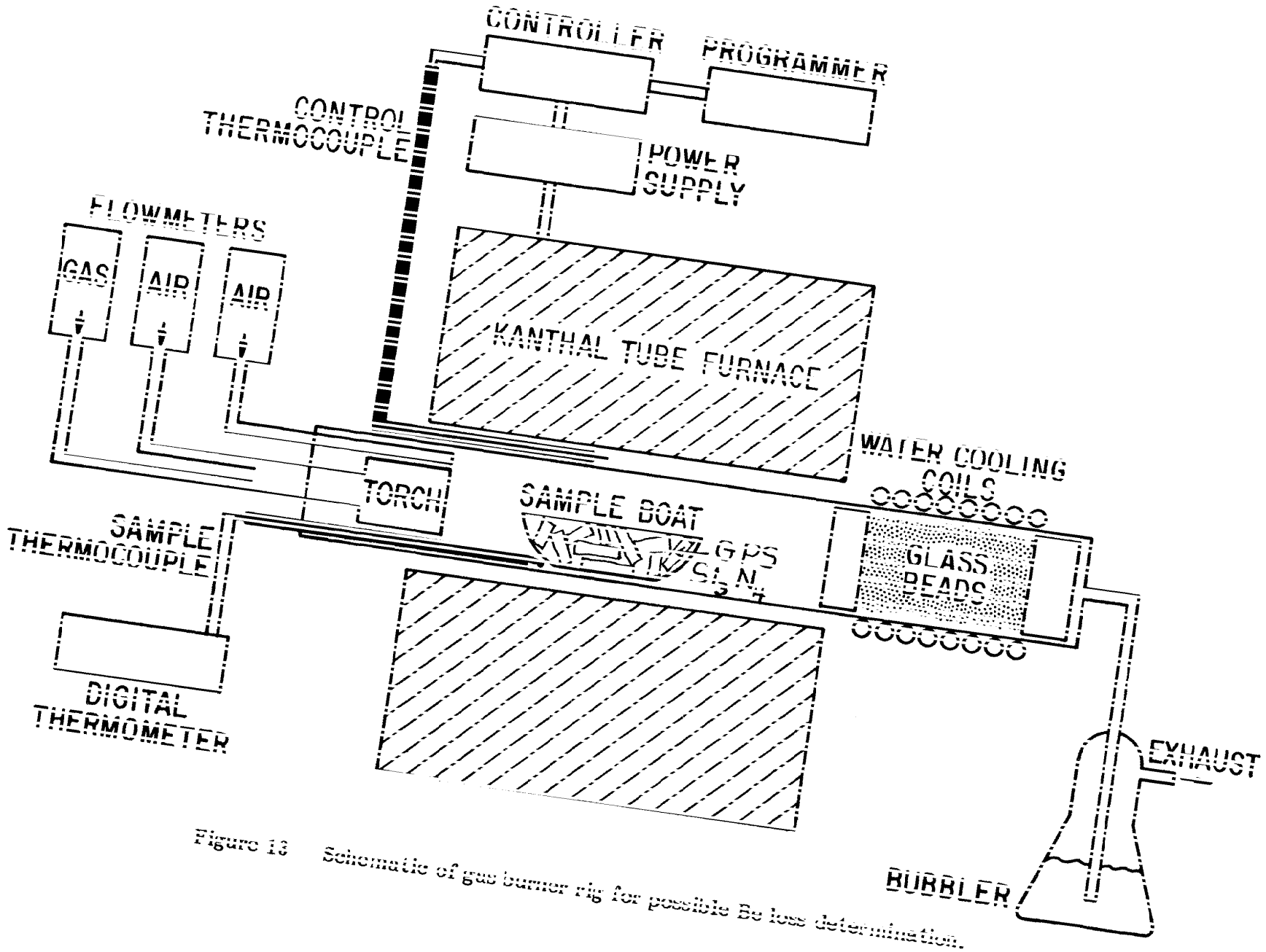

Figure 13 Schematic of gas burner rig for possible Be loss determination.

DISTRIBUTION LIST

No. of Copies	To
	Office of the Under Secretary of Defense for Research and Engineering, The Pentagon, Washington, DC 20310
1	ATTN: Mr. J. Persh
1	Dr. G. Gamota
12	Commander, Defense Technical Information Center, Cameron Station, Building 5, 5010 Duke Street, Alexandria, VA 22314
1	National Technical Information Service, 5285 Port Royal Road, Springfield, VA 22161
	Director, Defense Advanced Research Projects Agency, 1400 Wilson Boulevard, Arlington, VA 22209
1	ATTN: Dr. A. Bement
1	Dr. Van Reuth
	Battelle Columbus Laboratories, Metals and Ceramics Information Center, 505 King Avenue, Columbus, OH 43201
1	ATTN: Mr. Winston Duckworth
1	Dr. D. Niesz
	Deputy Chief of Staff, Research, Development, and Acquisition, Headquarters, Department of the Army, Washington, DC 20310
1	ATTN: DAMA-ARZ
1	DAMA-CSS, Dr. J. Bryant
	Commander, U.S. Army Medical Research and Development Command, Fort Detrick, Frederick, MD 21701
1	ATTN: SGRD-SI, Mr. Lawrence L. Ware, Jr.
	Commander, Army Research Office, P.O. Box 12211, Research Triangle Park, NC 27709
1	ATTN: Information Processing Office
1	Dr. G. Mayer
1	Dr. J. Hurt
	Commander, U.S. Army Materiel Development and Readiness Command, 5001 Eisenhower Avenue, Alexandria, VA 22333
1	ATTN: DRCDMD-ST
1	DRCLDC
	Commander, Harry Diamond Laboratories, 2800 Powder Mill Road, Adelphi, MD 20783
1	ATTN: Mr. A. Benderly
1	Technical Information Office
1	DELHD-RAE
	Commander, U.S. Army Missile Command, Redstone Arsenal, AL 35809
1	ATTN: Mr. P. Ormsby
1	Technical Library
	Commander, U.S. Army Aviation Research and Development Command, 4300 Goodfellow Boulevard, St. Louis, MO 63120
1	ATTN: DRDAV-EXT
1	DRDAV-QE
	Commander, U.S. Army Tank-Automotive Research and Development Command, Warren, MI 48090
1	ATTN: Dr. W. Bryzik
1	Mr. E. Hamperian
1	D. Rose
1	DRDTA-RKA, Dr. J. Chevalier
1	DRDTA-UL, Technical Library
	Commander, U.S. Army Armament Research and Development Command, Dover, NJ 07801
1	ATTN: Dr. G. Vezzoli
1	Technical Library
	Commander, U.S. Army Armament Materiel Readiness Command, Rock Island, IL 61299
1	ATTN: Technical Library
	Commander, Aberdeen Proving Ground, MD 21005
1	ATTN: DRDAR-CLB-PS, Mr. J. Vervier
	Commander, U.S. Army Mobility Equipment Research and Development Command, Fort Belvoir, VA 22060
1	ATTN: DRDME-EM, Mr. W. McGovern
1	DRDME-V, Mr. E. York
	Director, U.S. Army Ballistic Research Laboratory, Aberdeen Proving Ground, MD 21005
1	ATTN: DRDAR-TSB-S (STINFO)
	Commander, U.S. Army Test and Evaluation Command, Aberdeen Proving Ground, MD 21005
1	ATTN: DRSTE-ME
	Commander, U.S. Army Foreign Science and Technology Center, 220 7th Street, N.E., Charlottesville, VA 22901
1	ATTN: Military Tech, Mr. W. Marley
	Commander, Watervliet Arsenal, Watervliet, NY 12189
1	ATTN: Dr. T. Davidson
	Director, Eustis Directorate, U.S. Army Mobility Research and Development Laboratory, Fort Eustis, VA 23604
1	ATTN: Mr. J. Robinson, DAVDL-E-MOS (AVRADCOM)
1	Mr. C. Walker
	Chief of Naval Research, Arlingt
	Chief of Naval Research, Arlington, VA 22217
1	ATTN: Code 471
1	Dr. A. Diness
1	Dr. R. Pohanka
	Naval Research Laboratory, Washington, DC 20375
1	ATTN: Dr. J. M. Krafft - Code 5830
1	Mr. R. Rice
	Headquarters, Naval Air Systems Command, Washington, DC 20360
1	ATTN: Code 5203
1	Code MAT-042M
1	Mr. I. Machlin
	Headquarters, Naval Sea Systems Command, 1941 Jefferson Davis Highway, Arlington, VA 22376
1	ATTN: Code 035
	Commander, Naval Weapons Center, China Lake, CA 93555
1	ATTN: Mr. F. Markarian
	Commander, U.S. Air Force of Scientific Research, Building 410, Bolling Air Force Base, Washington, DC 20332
1	ATTN: MAJ W. Simmons
	Commander, U.S. Air Force Wright Aeronautics Laboratory, Wright-Patterson Air Dr. M. LindleyForce Base, OH 45433
1	ATTN: AFWAL/MLLM, Dr. N. Tallan
1	AFWAL/MLLM, Dr. H. Graham
1	AFWAL/MLLM, Dr. R. Ruh
1	AFWAL/MLLM, Mr. K. S. Mazdiyasni
1	Aero Propulsion Labs, Mr. R. Marsh
	National Aeronautics and Space Administration, Washington, DC 20546
1	ATTN: Mr. G. C. Deutsch - Code RW
1	Mr. J. Gangler
1	AFSS-AD, Office of Scientific and Technical Information
	National Aeronautics and Space Administration, Lewis Research Center, 21000 Brookpark Road, Cleveland, Cleveland, OH 44135
1	ATTN: J. Accurio, USAMRDL
1	Dr. H. B. Probst, MS 49-1
1	Dr. R. Evans
1	Dr. S. Dutta
1	Mr. C. Blankenship
	National Aeronautics and Space Administration, Langley Research Center, Center, Hampton, VA 23665
1	ATTN: Mr. J. Buckley, Mail Stop 387
	Department of Energy, Division of Transportation, 20 Massachusetts Avenue, N.W., Washington, DC 20545
1	ATTN: Mr. George Thur (TEC)
1	Mr. Robert Schulz (TEC)
1	Mr. John Neal (CLNRT)
1	Mr. Steve Wander (Fossil Fuels)
	Department of Transportation, 400 Seventh Street, S.W., Washington, DC 20590
1	ATTN: Mr. M. Lauriente
	National Research Council, National Materials Advisory Board, 2101 Constitution Avenue, Washington, DC 20418
1	ATTN: Dr. W. Prindle
1	R. M. Spriggs
	National Science Foundation, Washington, DC 20550
1	ATTN: B. A. Wilcox
	Admiralty Materials Technology Establishment, Polle, Dorset BH 6 6JU, UK
1	ATTN: Dr. D. Godfrey
1	Dr. M. Lindley

No. of Copies	To
	AiResearch Manufacturing Company, AiResearch Casting Company, 2525 West 190th Street, Torrance, CA 90505
1	ATTN: Mr. K. Styhr
	AiResearch Manufacturing Company, Materials Engineering Dept., 111 South 34th Street, P.O. Box 5217, Phoenix, AZ 85010
1	ATTN: Mr. D. W. Richerson, MS 93-393/503-44
	AVCO Corporation, Applied Technology Division, Lowell Industrial Park, Lowell, MA 01887
1	ATTN: Dr. T. Vasilos
	Carborundum Company, Research and Development Division, P.O. Box 1054, Niagara Falls, NY 14302
1	ATTN: Dr. J. A. Coppola
	Case Western Reserve University, Department of Metallurgy, Cleveland, OH 44106
1	ATTN: Prof. A. H. Heuer
	Cummins Engine Company, Columbus, IN 47201
1	ATTN: Mr. R. Kamo
	Deposits and Composites, Inc., 1821 Michael Faraday Drive, Reston, VA 22090
1	ATTN: Mr. R. E. Engdahl
	Electric Power Research Institute, P.O. Box 10412, 3412 Hillview Avenue, Palo Alto, CA 94304
1	ATTN: Dr. A. Cohn
	European Research Office, 223 Old Maryleborne Road, London, NW1 - 5the, England
1	ATTN: Dr. R. Quattrone
1	LT COL James Kennedy
	Ford Motor Company, Turbine Research Department, 20000 Rotunda Drive, Dearborn, MI 48121
1	ATTN: Mr. A. F. McLean
1	Mr. E. A. Fisher
1	Mr. J. A. Mangels
	General Electric Company, Research and Development Center, Box 8, Schenectady, NY 12345
1	ATTN: Dr. R. J. Charles
1	Dr. C. D. Greskovich
1	Dr. S. Prochazka
	General Motors Corporation, AC Spark Plug Division, Flint, MI 48556
1	ATTN: Dr. M. Berg
	Georgia Institute of Technology, EES, Atlanta, GA 30332
1	ATTN: Mr. J. D. Walton
	GTE Laboratories, Waltham Research Center, 40 Sylvan Road, Waltham, MA 02154
1	ATTN: Dr. C. Quackenbush
1	Dr. W. H. Rhodes
1	Dr. J. T. Smith
	IIT Research Institute, 10 West 35th Street, Chicago, IL 60616
1	ATTN: Mr. S. Bortz, Director, Ceramics Research
	Institut fur Werkstoff-Forschung, DFVLR, 505 Porz-Wahn, Linder Hohe, Germany
1	ATTN: Dr. W. Bunk
	Caterpillar Tractor Co., Solar Division, 2200 Pacific Highway, P.O. Box 80966, San Diego, CA 92138
1	ATTN: Dr. A. Metcalfe
1	Ms. M. E. Gulden
	Kawecki Berylco Industries, Inc., P.O. Box 1462, Reading, PA 19603
1	ATTN: Mr. R. J. Longenecker
	Martin Marietta Laboratories, 1450 South Rolling Road, Baltimore, MD 21227
1	ATTN: Dr. J. Venables
	Massachusetts Institute of Technology, Department of Metallurgy and Materials Science, Cambridge, MA 02139
1	ATTN: Prof. R. L. Coble
1	Prof. H. K. Bowen
1	Prof. W. D. Kingery

No. of Copies	To
	Midwest Research Institute, 425 Volker Boulevard, Kansas City, MO 64110
1	ATTN: Mr. Gordon W. Gross, Head, Physics Station
	Norton Company, Worcester, MA 01606
1	ATTN: Dr. N. Ault
1	Dr. M. L. Torti
	Pennsylvania State University, Materials Research Laboratory, Materials Science Department, University Park, PA 16802
1	ATTN: Prof. R. E. Tressler
1	Prof. R. Bradt
1	Prof. V. S. Stubican
	RIAS, Division of the Martin Company, Baltimore, MD 21203
1	ATTN: Dr. A. R. C. Westwood
	Rockwell International Corporation, Science Center, 1049 Camino Dos Rios, Thousand Oaks, CA 91360
1	ATTN: Dr. F. F. Lange
	Stanford Research International, 333 Ravenswood Avenue, Menlo Park, CA 94025
1	ATTN: Dr. P. Jorgensen
1	Dr. D. Rowcliffe
	State University of New York at Stony Brook, Department of Materials Science, Long Island, NY 11790
1	ATTN: Prof. Franklin F. Y. Wang
	United Technologies Research Center, East Hartford, CT 06108
1	ATTN: Dr. J. Brennan
1	Dr. F. Galasso
	University of California, Lawrence Livermore Laboratory, P.O. Box 808, Livermore, CA 94550
1	ATTN: Dr. C. F. Cline
	University of Florida, Department of Materials Science and Engineering, Gainesville, FL 32601
1	ATTN: Dr. L. Hench
	University of Michigan, Materials of Metallurgical Engineering, Ann Arbor, MI 48104
1	ATTN: Prof. E. E. Hucke
1	Prof. T. Y. Tien
	University of Newcastle Upon Tyne, Department of Metallurgy and Engineering Materials, Newcastle Upon Tyne, NEI 7 RU, England
1	ATTN: Prof. K. H. Jack
	University of Washington, Ceramic Engineering Division, FB-10, Seattle, WA 98195
1	ATTN: Prof. James I. Mueller
1	Prof. A. Miller
	Virginia Polytechnic Institute, Department of Materials Engineering, Blacksburg, VA 24061
1	Prof. D. P. H. Hasselman
	Westinghouse Electric Corporation, Research Laboratories, Pittsburgh, PA 15235
1	ATTN: Dr. R. J. Bratton
1	Mr. Joseph T. Bailey, 3M Company, Technical Ceramic Products Division, 3M Center, Building 207-1W, St. Paul, MN 55101
1	Dr. Jacob Stiglich, Dart Industries/San Fernando Laboratories, 10258 Norris Avenue, Pacoima, CA 91331
1	Dr. J. Petrovic - CMB-5, Mail Stop 730, Los Alamos Scientific Laboratories, Los Alamos, NM 87545
1	Mr. R. J. Zentner, EAI Corporation, 198 Thomas Johnson Drive, Suite 16, Frederick, MD 21701
	Director, Army Materials and Mechanics Research Center, Watertown, MA 02172
2	ATTN: DRXMR-PL
1	DRXMR-PR
1	DRXMR-PD
1	DRXMR-K
10	DRXMR-MC, Mr. G. E. Gazza

Army Materials and Mechanics Research Center
Watertown, Massachusetts 02172
SINTERING Si_3N_4 FOR HIGH PERFORMANCE THERMOMECHANICAL APPLICATIONS
W.D. Pasco and C.D. Greskovich
General Electric Company
Corporate Research and Development
Schenectady, New York 12301

AD _____

UNCLASSIFIED
UNLIMITED DISTRIBUTION

Key Words

Technical Report AMMRC-TR82-22, April 1982,
54 pp.-illus.-tables, Contract DAAG46-81-C-0029
Final Report, January 1981 - January 1982

Gas Pressure Sintering
Silicon Nitrides
Beryllium Compounds
Oxygen
High Temperature
Ceramic Materials

The gas pressure sintering (GPS) process for dense (>99%) Si_3N_4 containing ~7 wt% $BeSiN_2$ and 7 wt% SiO_2 as sintering aids was scaled-up to develop a property data base for use in thermomechanical applications at high (~1300 °C) temperatures. The fracture strength in 3-pt bend for test bars ~0.6 cm × 0.6 cm × 4.5 cm long was ~440 MNm^{-2} (63,700 psi) for a span length of 3.8 cm. There was little drop (<15%) in high temperature strength at 1400 °C in air. The creep resistance was outstanding at 1300 to 1400 °C, as evidenced by creep rates of ~$4 \times 10^{-5} h^{-1}$ for a stress of 207 MPa (30,000 psi) at 1400 °C and ~$2 \times 10^{-6} h^{-1}$ for a stress of 345 MPa (50,000 psi) at 1300 °C, and a total creep strain of 0.11% for a Si_3N_4 bar exposed for 650 h under an applied stress of 345 MPa at 1300 °C in air. The oxidation rates in oxygen were very low and were 7.4×10^{-13} and 2.1×10^{-12} $kg^2 m^{-4} s^{-1}$ at 1300 and 1405 °C, respectively.

Injection-molded Si_3N_4 of the General Electric composition could be sintered to 99.9% of its theoretical density by the GPS process.

A gas burner rig test conducted at 1200 °C for 525 h using an air-to-fuel ratio of 7.5:1 showed that the calculated amount of Be in the exhaust gas was very small, ~6 parts per billion.

Army Materials and Mechanics Research Center
Watertown, Massachusetts 02172
SINTERING Si_3N_4 FOR HIGH PERFORMANCE THERMOMECHANICAL APPLICATIONS
W.D. Pasco and C.D. Greskovich
General Electric Company
Corporate Research and Development
Schenectady, New York 12301

AD _____

UNCLASSIFIED
UNLIMITED DISTRIBUTION

Key Words

Technical Report AMMRC-TR82-22, April 1982,
54 pp.-illus.-tables, Contract DAAG46-81-C-0029
Final Report, January 1981 - January 1982

Gas Pressure Sintering
Silicon Nitrides
Beryllium Compounds
Oxygen
High Temperature
Ceramic Materials

The gas pressure sintering (GPS) process for dense (>99%) Si_3N_4 containing ~7 wt% $BeSiN_2$ and 7 wt% SiO_2 as sintering aids was scaled-up to develop a property data base for use in thermomechanical applications at high (~1300 °C) temperatures. The fracture strength in 3-pt bend for test bars ~0.6 cm × 0.6 cm × 4.5 cm long was ~440 MNm^{-2} (63,700 psi) for a span length of 3.8 cm. There was little drop (<15%) in high temperature strength at 1400 °C in air. The creep resistance was outstanding at 1300 to 1400 °C, as evidenced by creep rates of ~$4 \times 10^{-5} h^{-1}$ for a stress of 207 MPa (30,000 psi) at 1400 °C and ~$2 \times 10^{-6} h^{-1}$ for a stress of 345 MPa (50,000 psi) at 1300 °C, and a total creep strain of 0.11% for a Si_3N_4 bar exposed for 650 h under an applied stress of 345 MPa at 1300 °C in air. The oxidation rates in oxygen were very low and were 7.4×10^{-13} and 2.1×10^{-12} $kg^2 m^{-4} s^{-1}$ at 1300 and 1405 °C, respectively.

Injection-molded Si_3N_4 of the General Electric composition could be sintered to 99.9% of its theoretical density by the GPS process.

A gas burner rig test conducted at 1200 °C for 525 h using an air-to-fuel ratio of 7.5:1 showed that the calculated amount of Be in the exhaust gas was very small, ~6 parts per billion.

Army Materials and Mechanics Research Center
Watertown, Massachusetts 02172
SINTERING Si_3N_4 FOR HIGH PERFORMANCE THERMOMECHANICAL APPLICATIONS
W.D. Pasco and C.D. Greskovich
General Electric Company
Corporate Research and Development
Schenectady, New York 12301

AD _____

UNCLASSIFIED
UNLIMITED DISTRIBUTION

Key Words

Technical Report AMMRC-TR82-22, April 1982,
54 pp.-illus.-tables, Contract DAAG46-81-C-0029
Final Report, January 1981 - January 1982

Gas Pressure Sintering
Silicon Nitrides
Beryllium Compounds
Oxygen
High Temperature
Ceramic Materials

The gas pressure sintering (GPS) process for dense (>99%) Si_3N_4 containing ~7 wt% $BeSiN_2$ and 7 wt% SiO_2 as sintering aids was scaled-up to develop a property data base for use in thermomechanical applications at high (~1300 °C) temperatures. The fracture strength in 3-pt bend for test bars ~0.6 cm × 0.6 cm × 4.5 cm long was ~440 MNm^{-2} (63,700 psi) for a span length of 3.8 cm. There was little drop (<15%) in high temperature strength at 1400 °C in air. The creep resistance was outstanding at 1300 to 1400 °C, as evidenced by creep rates of ~$4 \times 10^{-5} h^{-1}$ for a stress of 207 MPa (30,000 psi) at 1400 °C and ~$2 \times 10^{-6} h^{-1}$ for a stress of 345 MPa (50,000 psi) at 1300 °C, and a total creep strain of 0.11% for a Si_3N_4 bar exposed for 650 h under an applied stress of 345 MPa at 1300 °C in air. The oxidation rates in oxygen were very low and were 7.4×10^{-13} and 2.1×10^{-12} $kg^2 m^{-4} s^{-1}$ at 1300 and 1405 °C, respectively.

Injection-molded Si_3N_4 of the General Electric composition could be sintered to 99.9% of its theoretical density by the GPS process.

A gas burner rig test conducted at 1200 °C for 525 h using an air-to-fuel ratio of 7.5:1 showed that the calculated amount of Be in the exhaust gas was very small, ~6 parts per billion.